Discovery of Latent Drivers from Double Mutations in Pan-Cancer Data Reveal their Clinical Impact

Bengi Ruken Yavuz[1], Chung-Jung Tsai[2], Ruth Nussinov[2,3], Nurcan Tuncbag[1,4,5,*]

[1]Graduate School of Informatics, Department of Health Informatics, Middle East Technical University, Ankara, 06800, Turkey

[2]Computational Structural Biology Section, Frederick National Laboratory for Cancer Research, National Cancer Institute at Frederick, Frederick, MD 21702, USA

[3]Department of Human Molecular Genetics and Biochemistry, Sackler School of Medicine, Tel Aviv University, Tel Aviv 69978, Israel

[4]Department of Chemical and Biological Engineering, College of Engineering, Koç University, Istanbul, Turkey

[5]School of Medicine, Koç University, Istanbul, Turkey

[*]To whom correspondence should be addressed at ntuncbag@ku.edu.tr

Abstract

Background. Transforming patient-specific molecular data into clinical decisions is fundamental to personalized medicine. Despite massive advancements in cancer genomics, to date driver mutations whose frequencies are low, and their observable transformation potential is minor have escaped identification. Yet, when paired with other mutations *in cis*, such 'latent driver' mutations can drive cancer. Here, we discover potential 'latent driver' double mutations.

Method. We applied a statistical approach to identify significantly co-occurring mutations in the pan-cancer data of mutation profiles of ~80,000 tumor sequences from the TCGA and AACR GENIE databases. The components of same gene doublets were assessed as potential latent drivers. We merged the analysis of the significant double mutations with drug response data of cell lines and patient derived xenografts (PDXs). This allowed us to link the potential impact of double mutations to clinical information and discover signatures for some cancer types.

Results. Our comprehensive statistical analysis identified 228 same gene double mutations of which 113 mutations are cataloged as latent drivers. Oncogenic activation of a protein can be through either single or multiple independent mechanisms of action. Combinations of a driver mutation with either a driver, a weak driver, or a strong latent driver have the potential of a single gene leading to a fully activated state and high drug response rate. Tumor suppressors require higher mutational load to coincide with double mutations compared to oncogenes which implies their relative robustness to losing their functions. Evaluation of the response of cell lines and patient-derived xenograft data to drug treatment indicate that in certain genes double

mutations can increase oncogenic activity, hence a better drug response (e.g. in PIK3CA), or they can promote resistance to the drugs (e.g. in EGFR).

Conclusion. Our comprehensive analysis of same allele double mutations in cancer genome landscapes emphasizes that interrogation of big genomic data and integration with the results of large-scale small-molecule sensitivity data can provide deep patterns that are rare; but can still result in dramatic phenotypic alterations, and provide clinical signatures for some cancer types.

Keywords: mutation doublets, molecular signatures of cancer, latent drivers, cancer genome analysis, passenger mutations

Background

Cancer is a disease of uncontrolled cell proliferation driven by molecular alterations. The impact of these alterations diffuses into the molecular interaction network and changes signaling pathways and transcriptional regulation in the cell. Not all alterations equally contribute to growth advantage of cancer cells. Some mutations are drivers; others are passengers [1]. Whereas it is generally believed that passenger mutations do not bestow proliferative effects on the disease phenotype, their properties and possible roles are not fully understood [2]. Comprehensive screening of thousands of p53 mutations and phenotypic characterization of these mutations have shown that mutations that maintain wild-type functionality of p53 are unlikely to be cancer drivers [3]. However, cancer genomics and evolutionary studies suggest that the accumulation of ‘slightly’ deleterious passenger mutations can slow cancer progression and this could be exploited for therapeutic purposes [4]. Lately, another class of mutations was

63 defined, dubbed “latent” or “mini-drivers” [5-7]. Latent mutations may assume a driver-like
64 behavior yet were not identified as drivers per se. Latent drivers emerge during cancer evolution
65 and their detection may help forecast cancer progression and improve personalized treatment
66 strategies [6]. Driver mutations are classified into three types, strong driver, driver and weak
67 driver. As for latent drivers, there are strong latent and weak latent drivers. Curated driver genes
68 and mutations have been deposited in multiple databases [8-10]and used by multiple research
69 groups to develop computational approaches to predict driver genes and driver mutations [11-
70 16]. These methods, including the frequency-based methods, subnetwork identification methods,
71 and 3D mutation search methods, have been comprehensively compared [17-19]. One of the
72 concerns with frequency-based approaches is that prohibitively large sample sizes are needed to
73 identify infrequently mutated driver genes. Thus, in frequency-based approaches, there is a risk
74 of generating biased results due to background mutation rates [20]. Large databases catalog
75 cancer driver genes and driver mutations and help in understanding the mechanism behind
76 tumorigenesis. However, frequency-based approaches fail in the identification of rare drivers
77 which can be tissue-specific [21]. A recent multidimensional analysis of cancer driver genes in
78 IntOGen showed that some drivers are cancer-wide whereas others are specific to a limited
79 number of cancer types [14].

80 Even a single mutation in a gene can be considered as a prognostic marker and change the global
81 genome and protein expression, eventually altering the signaling pathways [22]. However, it has
82 been estimated that the contribution of a single driver mutation to cancer progression is very
83 small and needs additional mutations over time [23]. Despite DNA repair, somatic mutations
84 accumulate and different genotypes in individual tissues are generated. This mechanism, called
85 ‘somatic mosaicism’, offers driver or synergistic mutations an advantage in cancer cells [24].

Recently, the combination of single frequent mutations with a rare, or weak mutation in the *same* gene was shown to have a significant advantage in tumor progression and influence treatment response. These double mutations *in cis* in PIK3CA were shown to be more oncogenic, and more sensitive to an inhibitor compared to a single mutation [25]. A recent work cataloged 'composite mutations' of *multiple* genes – i.e. acting through same proteins – having more than one non-synonymous mutation in the same tumor [26]. Saito et al demonstrated the functional implications of multiple driver mutations in the same oncogene with an emphasis on PIK3CA [27]. Analysis of the rare mutations in cancer patients revealed known and hidden onco-drivers that are mutually exclusive in the same pathway suggesting epistatic mechanisms [28]. Many approaches are based on the principle that functionally-related genes have similar profiles of epistatic interactions [29]. One proposed explanation, typically for mutations in the same cellular pathway, involves functional redundancy. After a pathway has been mutated once, there is no evolutionary benefit to the clone from additional mutations in that pathway [29, 30].

Here, aided by informatics techniques, we systematically screen somatic mutations in pan-cancer data across ~80,000 patient tumors. We aim to find co-occurring patterns that are predominantly present in specific tissues and tumor types. Our screening reveals tumor-type specific double mutations on the same gene which may promote tumorigenesis and alter the response to treatments. It also reveals that tumors having at least one double mutations pair can lead to changes in response to drugs. We cataloged the components of double-mutations as latent mutations if their co-occurrence is significant and not yet labeled as a cancer driver. This led us to uncover 113 latent driver mutations. The oncogenic activation of a gene is through either single or multiple independent mechanisms of action. We present these different mechanisms through the same gene double mutations. Although the existence of a set of driver genes is

considered cancer-wide, we show that having double mutations on those genes is cancer-specific. Same gene double mutations are relatively rare; however, their impact is elevated in tumor progression.

Methods

Data collection and Processing

All available somatic missense mutation profiles are downloaded from two sources, The Cancer Genome Atlas (TCGA) and the AACR launched Project GENIE (Genomics Evidence Neoplasia Information Exchange) [31-33]. The TCGA mutation annotation file contains more than 11,000 human tumors across 33 different cancer types. The GENIE mutation file (Release 6.2-public) contains 70679 samples across 671 cancer subtypes under Oncotree classification. The GENIE cohort contains multiple tumor barcodes belonging to the same tumor type. In such a case only one primary tumor barcode is kept for further analysis. We continued the analysis with 78837 samples from 671 cancer subtypes and 34 tissues (including UNKNOWN and OTHER categories).

Identification of Significant Double Alterations

The total number of mutations is 1638191 in 19443 genes. We only evaluated dual combinations of 21983 (on 5062 genes) of these alterations observed on at least 5 tumors and constructed binary combinations of them. Then we created a contingency table for each combination of tumor numbers having both alterations, only the first or second alteration and none of those two alterations. Based on the contingency table, we calculated the p-value by using Fisher Exact Test with the formula below:

$$\frac{\binom{a+b}{a}\binom{c+d}{c}}{\binom{a+b+c+d}{a+d}} \quad (1)$$

where a is the number of tumors having both alterations, b is the number of tumors having only the first alteration, c is the number of tumors having only the second alteration and d is the number of tumors not having these two alterations.

228 significant pairs and 227 non-significant pairs were decided using the Fisher Exact Test for p=0.05. We used the Catalog of Validated Oncogenic Mutations from the Cancer Genome Interpreter [10] to label dual mutation components: if a mutation is among the 5601 driver mutations, we label it as known driver (D), otherwise potential latent driver (d). We then classified a known driver mutation as a driver if it is present in more than 500 tumors; otherwise, it is a weak driver. Similarly, we dubbed a potential latent driver mutation as a strong latent driver if it is present in more than 10 tumors; otherwise, we classified it as a weak latent driver.

Additionally, double mutations are annotated based on their functions, domains, chemical properties and structural proximity (see Supplementary Text)

Survival Analysis

For survival analysis, 10336 patients in MSK impact 2017 and 11160 patients in TCGA and their overall survival status are used [31, 33]. We compared survival times of tumor groups with significant same/different gene double mutations and single mutations in a specific cancer subtype. The first group is the union of patients with significant doublets whereas the second is the union of patients that carry only one component of these significant double mutations. Then

we gathered overall survival times (time in months) and vital status (1: Deceased, 0: Alive) of these patients for survival analysis.

We utilized the "survival" library of R to do Kaplan Meier Survival Analysis of double and single mutant groups. The survival probability at any particular time is calculated by the formula given below [34]:

$$S_t = \frac{(Number\ of\ subjects\ living\ at\ the\ start) - (Number\ of\ subjects\ )}{Number\ of\ subjects\ living\ at\ the\ start} \quad (2)$$

Oncoprint Maps

To reveal mutual exclusivity and co-occurrence patterns between double mutations we plotted oncoprint maps by using ComplexHeatmap package of R [35].

Cell Line Network Construction

We obtained a list of cell lines with the dual mutations from Cell Model Passports and their drug response information from CancerrxGene [36, 37]. We also extracted information about drug targets and target pathways. We used 2 different approaches to select drugs for PTEN, APC, and PIK3CA dual mutant cell lines: if a drug is in the gray zone (|z-score|<=2) in the single mutant cell lines but gives a significant drug response in a dual mutant cell line (|z-score|>2). If there is a single mutant cell line that is sensitive (or resistant) to the drug but the dual mutant cell line gives an opposite response to the drug. (Drug response flips sensitive into resistant or resistant into sensitive between single and dual mutant cell lines).

For EGFR we selected drugs that give significant drug response either in the single or dual mutant cell line. Then we formed networks connecting mutations to cell lines, cell lines to drugs, and drugs to their target pathways.

Patient-Derived Xenograft Analysis

We used the mutation profiles, transcriptomic data and drug responses of patient-derived xenografts in [38]. We determined xenografts harboring significant doublets. Then, we compared changes in tumor volumes of single and dual mutant xenografts for the untreated and drug-treated cases (single mutation is part of a significant dual mutation). We preferred to specify the time intervals in multiples of 5. When a given timepoint is not a multiple of 5, we used linear interpolation between two nearest numbers containing a multiple of 5.

$$Vol_i = Vol_{i-1} + \frac{t_i - t_{i-1}}{t_{i+1} - t_{i-1}}(Vol_{i+1} - Vol_{i-1}) \quad (6)$$

where t_i is a timepoint that is multiple of 5 between the given timepoints t_{i-1} and t_{i+1} and Vol_i is the volume (mm^3) at timepoint i.

Results

Discovery of Latent Drivers through Double Mutations

The availability of a vast amount of pan-cancer genomic data helps to find mutational patterns that can be signatures of the specific tumor tissues or cancer types. Multiple mutations in a single gene rarely co-occur in patient tumors. However, when they are together, they may cause dramatic phenotypic differences [25-27]. For example, dual mutations in PIK3CA increase the sensitivity to PI3K inhibitors in breast cancer [25], while dual mutations in EGFR predominantly

exist in lung cancer [39]. A strong driver may couple with a weak driver or a latent driver to increase the pathological impact of the alterations. This pattern also gives insight into the latent drivers that are context specific. We exploited the dual mutations to discover latent drivers. For this purpose, following the Oncotree classification we obtained and cataloged missense mutation profiles of ~80,000 tumors from TCGA and GENIE Pan-Cancer datasets from 34 main tissues and 672 cancer subtypes including tissues tagged as Unknown and Other (Figure 1A). Collecting all missense mutations on each gene and counting their pairwise combinations result in 228 significant double mutations (p-value < 0.05, Fisher exact test). Especially, when single mutations across patient tumors are systematically reduced in the co-occurring mutation patterns, the double mutations are revealed to be cancer specific. We also assembled tissue-specific sets of double alterations since tissues differ in sample size and are enriched in different genes and mutations. As shown in Figure 2A, co-occurring double mutations on the same gene are relatively rare, with varied frequencies across tissues. In some cancer tissues, doublets are present on the same gene in up to 10% of the patient tumors. However, same gene doublets are either extremely rare or not present in other tissues, such as the pancreas, ovary, liver, kidney, biliary tract. Same gene double mutations accumulate on 35 genes in the pan-cancer dataset of which 20 genes are tumor suppressors (TSG), 12 are oncogenes (OG) and the rest labeled as both.

Recently, the frequency of driver genes was analyzed together with the maximum prevalence of their mutations, distinguishing cancer-specific drivers versus cancer-wide drivers [14]. We applied a similar analysis to our dataset composed of double mutations on the same gene where we obtained the ratio of the number of tissues carrying double mutations (T_{double}) and single mutations (T_{single}). We also calculated the prevalence of double mutations compared to single

mutations. As a result, although some genes and their single mutant states have been previously cataloged cancer-wide, we found sets of double mutations that are cancer tissue-specific. Examples include double mutations in PTEN, EGFR, and KRAS (Figure 1B).

We retrieved the known driver mutations from the Cancer Genome Interpreter database to evaluate if the double mutations are composed of known drivers or other mutations that are not cataloged as drivers but can be considered as 'potential latent driver' mutations. In a doublet, the components can be known drivers or potential latent drivers, so each doublet is cataloged as DD, Dd and dd. That is, DD is a known driver-known driver doublet, Dd is a known driver-potential latent driver and dd is a doublet consisting of two potential latent drivers. Among the 228 same gene double mutations, there are 115 DD, 28 Dd, 85 dd where the mutations that are not catalogued as driver are potential latent drivers (the 228 same gene double mutations are composed of 91 known major drivers, 113 potential latent drivers). Thus, our analysis can capture rare mutations that are potential latent driver candidates. We observe that oncogenes have significantly more DD mutations than tumor suppressors (p-value $< 10^{-4}$), although their background probability to have a double mutation is similar (Figure 1C). This result implies that becoming more oncogenic requires mostly co-occurrence of two frequent mutations while suspending tumor suppressor activities may involve rare mutations coming together.

Tumor suppressor genes have 131 double mutations in 883 patient tumors and oncogenes have 91 double mutations in 1000 patient tumors. Patient tumors that have at least one double mutation in any TSG have a significantly higher passenger mutation load compared to patient tumors having at least one double mutation in an oncogene (p-value $< 10^{-11}$, Figure 1D). These results imply that double mutations are very rare. Especially tumor suppressor genes require a very high mutation load for two coexisting mutations in a single gene. Based on the mutation

load, and in line with our previous result, loss of function through double mutations in TSGs requires considerably higher mutational load compared to gain of function in oncogenes.

Known driver mutations have a higher frequency than potential latent driver mutations (Figure 1E). The median values of tumor counts for known driver and potential latent driver mutations are 170 and 35.5, respectively (p-value < 5x10-20). Potential driver mutations are relatively rare, and their pathological impact can be dramatic when they couple with another mutation. Therefore, we cataloged all potential latent driver mutations that contribute to a significant doublet in the same gene as strong or weak latent drivers. The list of 113 latent drivers is given in Table S1.

Next, we followed a bottom-up approach to obtain the spatial, chemical, and pathway level organization of the double mutations. We used the pan-cancer mutation clusters deposited in 3DHotspot where each cluster represents the set of mutations that are spatially close to each other [40]. We found that components of the doublets in the same gene are usually spatially distant from each other. The simultaneous presence of spatially close two strong driver mutations is very rare in a patient tumor. However, some weak drivers are proximal to either a strong driver or another weak driver, as in the cases of mutations at positions 711, 714, 715 in BRAF. Spatially close residues may form potent allosteric couples, which may enhance proliferation.

Analysis of the chemical class of doublets in oncogenes and tumor suppressor genes harboring the same gene doublets revealed that Charged-Polar and Hydrophobic-Charged switches are more dominant among tumor suppressors and oncogenes respectively (Figure 1F). Double mutations are either located in flexible or hinge or disordered regions or in different domains (Supplementary Text, Figure S1A). Components of each double are annotated in different molecular functions (Supplementary Text, Figure S1B).

Doublets on the Same Gene are Rare, but are a Signature for Some Cancer Types

Figure 2A illustrates the tissue-specific prevalence of double mutations in the same gene. TP53 and its double mutations are cancer wide. A recent study verified that PIK3CA double mutations *in cis* increase oncogenicity and sensitivity to PI3Kα inhibitors [25]. In our dataset, PIK3CA double mutations are also quite common in breast and uterus tumors. In the uterus, PIK3CA mutations are more inclined to constitute double mutations (around 90%). Among lung tumors, EGFR and bowel tumors APC double mutations are ahead by far. Bowel, breast, and lung tissues are enriched with double mutations on specific genes whereas brain tissue has significant double mutations in multiple genes such as BRAF, FBXW7, KDM5A, STAG2, TP53, TSC1. LUAD (Lung Adenocarcinoma) is enriched with EGFR dual mutations. 90% of the EGFR mutations are in more than 160 tumors. COAD (Colon Adenocarcinoma) is enriched with APC and PTEN dual mutations. We note that PIK3CA double mutations are relatively more dominant in BRCA, COAD, and UCEC subtypes (Figure 2B). A set of known driver mutations, for example in KRAS and IDH1 are usually present as single mutations but are frequently paired with mutations in other genes. The most frequent IDH1 mutation occurs at position 132 located in the interface of its homodimer [41].

The most frequent mutation, $KRAS^{G12D}$, is rarely coupled with another mutation in KRAS. The mutational mosaic of KRAS is distinguishable in different cancer types. $KRAS^{G12D}$ is predominantly present in pancreatic and colorectal cancers [42]. KRAS mutations are context-specific and a mutation may act in different cancers. However, among this limited number of KRAS double mutations, $KRAS^{G12D/A149T}$ accumulates in lung tissue and only exists in primary tumors in our dataset. $KRAS^{A146T}$ promotes opening of Switch I in GEF mediated GDP-GTP nucleotide exchange whereas $KRAS^{G12D}$ abolishes GAP-mediated hydrolysis [43].

Figure 2C illustrates some sequence details. In APC, EGFR, PTEN, and TP53 the diversity of the double mutations is limited, but this is not the case in PIK3CA and BRAF. Among them, $BRAF^{V600E}$, a strong driver, is rarely coupled with another BRAF mutation, but the rest are (Figure S2A). Other BRAF mutations such as at 711, 714, 715, and 721 are close to each other and coupled in a set of patients, especially in brain tissue (Figure S2B and S2C).

Another interesting case is the double mutations in the cohesin complex. Mutated cohesin can enhance Wnt signaling by stabilizing beta-catenin [44]. Targeting Wnt signaling in cohesin mutant cancer cells was proposed as a novel therapeutic strategy. Double, even multiple mutations in the components of the cohesin complex (Figure S3A) in the same tumor may dramatically increase Wnt signaling. In Figure S3B, we notice that STAG2 double mutations accumulate in the brain, RAD21 and SMC3 double mutations are prominent in lymph and myeloid tissues.

The Clinical Impact of Double Mutations in PIK3CA

PIK3CA is a large protein with drivers e.g. H1047R, E545K and weak drivers such as R88Q, E453K, M1043I. It is the second (or third) most highly mutated protein and its number of double mutations is also relatively higher than other proteins. The pathological impact of a single driver may be insufficient. Full activation of oncogenic PIK3CA is through two drivers acting in different, albeit complementary mechanisms. One well-known example is H1047 and E545 double mutations enhancing proliferation [45]. However, E545 and E542 double mutations do not make PIK3CA reach the fully activated level. Also, the combination of two strong latent driver mutations – but not two weak – can act like a driver mutation.

In our dataset of significant double mutations, 46 of the 228 are in PIK3CA. Enhanced activation of PIK3CA via dual mutations is shown in Figure 3A, where most of them are composed of one frequent and one rare mutation. Our frequency-based analysis revealed that P104, E726 and M1004 might be a strong latent drivers coupled with a driver mutation. PIK3CA double mutations are also tissue- and context-specific as shown in Figure 3B. Most are in breast tissue. An exception involves R88Q doublets which are depleted in breast but frequent in uterus tumors. Their structural location is shown in Figure 3C. Kinase mutations work by destabilizing the inactive or stabilizing the active state. These are better captured by their detailed conformational consequences. The mechanisms of activation of PI3Kα by these driver mutations have been recently worked out [45-47]. Unsurprisingly, considering their diverse mechanisms of action no clear trend is observed in the calculated folding free energy (ΔΔG) upon double or single mutation with DynaMut [48] (Suppl. Text and Figure S4). If the components of double mutations act via distinct mechanisms, the additivity of their activation potential is high; otherwise the additivity is low as in the E545/E542 example where the mutations execute the same mechanism of action.

The impact of co-occurring mutations in the same gene is mostly additive but can be also cooperative. There are seven allosteric mutations at positions 83, 88, 365, 539, 542, 603, 629 in PIK3CA in BRCA as cataloged in Allosteric DB [49]. We found 23 significant double mutations in PIK3CA in the BRCA subtype of breast tumors. Dual mutations $PIK3CA^{1047/88}$, $PIK3CA^{1047/539}$, $PIK3CA^{1047/539}$ are composed of one known driver (at position 1047) and one weak driver mutation ($PIK3CA^{88}$ and $PIK3CA^{539}$) which are allosteric mutations. Their effects are additive.

To further evaluate the double mutations, we used cancer cell lines from the DepMap project and patient-derived xenograft (PDX) samples in [38]. In both datasets, mutation profiles and response to drug treatment information are available. Additionally, we used the temporal data on tumor volume growth in PDX samples in untreated conditions and drug-treated conditions.

We found two breast cancer cell lines belonging to the BRCA subtype: BT-20 has a double mutation PIK3CA$^{1047/539}$ and Cal-148 has PIK3CA$^{1047/350}$. H1047R is a frequent driver. However, 539 and 350 are rare mutations in the Pan-cancer data, making them weak drivers. To explore the impact of the double mutations in terms of drug response, a network of cell lines to drugs and target pathways is constructed (Figure 3D) where drugs are linked to each cell line which has altered response compared to their single mutation counterparts. Cal-148, which has PIK3CA$^{1047/350}$, is more sensitive to drugs targeting the PI3K/mTOR pathway compared to the single mutant cell lines. Indeed, we found a difference in the response to PIK3α inhibitors in double-mutant cell line BT-20 which is more sensitive to this class of inhibitors compared to single mutant cell line counterparts (p-value=0.015). Additionally, an evaluation of other classes of inhibitors showed that the PIK3γ inhibitor CZC24832 does not work on single mutant MFM-223, but double mutant BT-20 is sensitive to it (Figure 3E).

We retrieved PDXs having double mutations in PIK3CA to explore the tumor volume changes and drug responses compared to single mutant PDXs. Properties of the patient tumors can be maintained in xenografts and can help assess the impact of double mutations. We found three PDXs having double PIK3CA mutations (726/1047, 88/542, 88/1025). In PDX X-2524 H1047R/E726K, a strong driver/strong latent driver combination, the volume change of the tumor between days 0 and 10 is more than 1700 mm^3, while single mutant tumors X-3077 and X-3078 (with mutation H1047R) have volume change of ~200 mm^3 in the first 10 days reaching

~400 mm^3 at around 35 days (Figure 3F). H1047R/E726K tumors grow significantly faster compared to the single mutant case.

We analyzed the effects of drugs on tumor growth of these three PDX tumors. We observed that BYL-719 (Alpelisib), a selective PI3Kα inhibitor, diminishes tumor volume by 88% (around 1600 mm^3) in the first 10 days in the double mutant in the xenograft (X-2524) (Figure 3G). Because the tumor volume growth is mild in the single mutant xenografts X-3077 and X-3078 the volume difference between the initial tumor and after 10 days of treatment with BYL-719 is not as high as in dual mutant X-2524. Also, we noticed that BYL-719 treatment combined with LJM716, an anti-HER3 monoclonal antibody, is more effective in reducing tumor volume than BYL-719 treatment alone (Figure 3H). Dual mutation E726/H1047 makes the tumor grow significantly faster compared to the single mutant case. The double mutant tumor is also more sensitive to PI3K inhibitors.

However, not all doublets increase the PIK3CA oncogenic activity. For example, the impact of double mutation R88/T1025 (a combination of weak drivers) differs from E726K/H1047R in the screened PDX tumors. The growth rate of the tumor with R88/T1025 is slower than the tumor having a single mutation (at position 88). The tumor with only R88 is more responsive to PI3K inhibitors compared to that with R88/T1025 (Figure S5A-H).

Linking Double Mutations to Clinical Data Using Cancer Cell Lines and Xenografts

Dual mutations may increase the activation strength and enhance drug response. In Figure 4 we show driver mutations combined with weak drivers or strong latent drivers in EGFR, BRAF,

APC and PTEN. Below, we probe PTEN, APC and EGFR double mutations with respect to drug treatments.

We screened all significant doublets across cell lines and PDX tumors. Double mutations are rare in the patient tumor samples and in cancer cell lines. Treatment data of patients are limited. Therefore, we aim to associate each marker double mutation with the cell lines or PDXs and assess their phenotypic impact through drug response data compared to their single mutant counterparts. In this way, we can assess the clinical impact of the same gene dual mutations and link the dual mutation patterns to drug response. We used the DepMap dataset together with Cell Model Passports to retrieve the mutational profile of cancer cell lines and the response to a panel of hundreds of drugs. We notice the same pattern: despite scanning hundreds of cancer cell lines, double mutations on the same gene are rare. In Figure 5, double mutations are linked to cell lines having the same pair, and cell lines are linked to drugs causing a significant response. These links are represented as a network of mutations, associated cell lines, and drugs. We listed some of the striking results on how dual mutations can alter the response to the drug in the same tissue.

Among 228 same gene mutations only 17 doublets match with one or more cell lines in Cell Model Passports [36]. We constructed a network by using Cytoscape [50] with 4 different node types, mutations (components of a double mutation), cell lines, drugs, and drug target pathways. In the same gene double mutation network, there are 22 mutations, 19 cell lines, 206 drugs, and 22 drug target pathways nodes with 548 edges between them. In Figure 5A, we show the prevalence of the same gene dual mutations in corresponding tissues of the cell lines. These are consistent with the patient tumor doublets obtained in the previous section.

One example is $EGFR^{L858/T790}$ doublet, a combination of two driver mutations (Figure 4A), in one cell line (NCI-H1975) of lung cancer. H3255 cell line has only one mutation at position

L858 in EGFR (Figure 5B). Both mutations are on the tyrosine kinase domain to which the RTK inhibitors bind (PDB: 4IF23, Figure 5C). However, response to the inhibitors is significantly different in cell line with dual mutant EGFR which is more resistant compared to the single mutant cell line (p-value=0.01, Figure 5D).

BRAF has multiple double mutations (Fig. 4B). The most significant doubles contain the V600 strong driver and one of the strong latent drivers (I710, L711, I714, E715, L721). E715 is in the interface of the BRAF homodimer and the other strong latent drivers are in the same 3D cluster with E715. These mutations are not annotated based on their clinical or kinase activity; however, contributing to a significant double mutation make them strong latent driver candidates. They can be further analyzed based on their mechanism of action complementing V600. The mechanisms of BRAF mutations were classified into those signaling as active monomers, those acting as constitutive active dimers, and those having impaired/dead kinase activity [51]. Despite being very rare in our dataset, we have three cases of impaired/dead mutations paired with other classes: $BRAF^{G469/K601}$, $BRAF^{G466/L597}$, and $BRAF^{G466/V600}$. Another rare double mutation is $BRAF^{L597/K601}$. The double mutation components lead to a constitutively active dimer, independent of Ras. The mutations may increase Raf affinity. A combination of strong latent drivers located at or close to the dimer interface can fit into this activation mechanism. To identify these pairs a larger dataset is necessary, but still we can identify some rare doubles that need clinical evaluation.

A second example involves PTEN (Figure 5E). $PTEN^{R130/R233}$ and $PTEN^{R130/F341}$ doublets, both composed of a driver and a weak driver mutation (Figure 4C), exist in two cell lines which differ in response to drugs as compared to their single mutant counterparts. Although single mutant PTEN is resistant to drugs targeting ERK/MAPK signaling, cell lines having dual mutant PTEN

are sensitive to these drugs. Additionally, cell line SNU-81 having $PTEN^{R130/R233}$ becomes resistant to genome targeting drugs compared to single mutant cell lines.

The lower panel of Figure 5F presents APC dual mutations with associated cell lines. The subnetwork shows that cell line SW837 carrying dual mutant APC (R1450*/R213*, a combination of weak drivers (Figure 4D) becomes resistant to drugs targeting PI3K/TOR signaling when compared to the single mutant cell lines. Additionally, in the patient-derived xenograft dataset from [38], there is one xenograft carrying R1450*/R876* dual mutation (a combination of two weak driver mutations), model id X-1290, and one carrying single R1450* mutation, model id X-1173. We compared volume changes of these xenografts. For the dual mutant xenograft X-1290 is ~1500 mm^3 in the first 30 days and for the single mutant xenograft X-1173 ~1200 mm^3. The dual mutant xenograft does not encounter any tumor volume change during the first 70 days when treated with Cetuximab, an EGFR inhibitor, while the single mutant xenograft keeps growing around 900 mm^3 during the first 15 days (Figure S6A-D).

Despite the small number of patients with follow-up information, Kaplan-Meier survival analysis comparing single and same gene double mutant patient groups demonstrates a significant difference between the two groups. Patients with double mutant PIK3CA (H1047/R88) and APC (R876/T1556) have worse survival than their single mutant counterparts. On the other hand, the patient group with PTEN double mutation (R130/R173) has a better survival than the single mutant group (Figure S7A-C).

Discussion

The highly heterogeneous molecular profiles of tumors compel comprehensive studies to reveal the underlying patterns resulting in their dramatic phenotypic differences. Distinguishing cancer drivers from passengers has been one of the key objects of such studies. Here we scan the cancer genome landscapes aiming to identify latent drivers. We designed this study to discover latent driver mutations based on the hypothesis that some rare, or weak mutations can cooperate with other, *in cis* mutations, to enhance the oncogenic signal. In terms of population of conformations, conceptually, a strong driver mutation is close to a fully activated state with more than 90% of the population in the active state. However, the contribution of other types of drivers in the gene toward reaching a fully activated state can differ. For example, the contribution of a driver to the active state population can be between 50-75%, that of a weak driver is around 50% and the contribution of a strong latent driver is above 25%. This implies multiple mechanisms of action of double mutations relating to the combination of a driver mutation with either driver, weak driver, or strong latent driver. Latent driver mutations are protein context-specific having driver-like behavior but not identified as driver. We identified 228 significant, same gene double mutations which are composed of mostly one rare and one frequent mutation. Components of these double mutations are labelled as latent drivers if they have not been previously cataloged as driver. We newly cataloged 113 latent drivers. Despite being cancer-wide on their own, coupling with another mutation increases the cancer-type specificity and decreases the prevalence of these double mutations. The mutation load of tumors having a doublet in a tumor suppressor is significantly higher than in an oncogene, indicating their relative robustness to functional loss.

With the sparsity of patient treatment datasets, cell lines or patient-derived tumor xenografts are a useful clinical interpretation resource. We found significant differences in the response to PI3K inhibitors in double mutant PIK3CA samples which is in line with the recent work by Vasan et al

[25, 27]. Additionally, tumor growth is extremely fast in double mutant PIK3CA compared to the single mutant. This phenotypic difference has been shown by Vasan et al for the couples of potential latent driver PIK3CA mutations E726, and weak drivers E453, M1043 with known driver mutations E542, E545, and H1047. Recent mechanistic studies suggest that the increased gene activity or acquired drug resistance is due to the mutation combinations. Zhang et al. [45] suggested that combinations of strong and weak drivers can enhance PI3K activity and explain the phenotypic differences in PIK3CA double mutant tumors, that we observed prominently in breast and uterus tumors. Here we further extended the analysis to combinations of less frequent mutations not catalogued as driver, which we view as potential latent drivers. Among them doubles with mutation at position R88 are depleted in breast but not in uterus, suggesting that potential latent driver mutations pairing with the mutation R88 are important signatures of uterus tumors.

Not limited to PIK3CA, numerous other significant double mutations with possible prognostic or therapeutic impact have also been identified (i.e. APC doublets in the bowel, EGFR in the lung in line with previous studies [26]). Some have not been previously analyzed clinically but have potential impact on drug response. For example, APC R1450/R876 double mutation results in significant sensitivity to cetuximab compared to single mutant APC R1450 in PDXs. On the other hand, cell lines having APC R1450/R213 doublet became resistant to PI3K/mTOR signaling inhibitors. Our approach also identified several rare same gene doublets, like the ones on cohesion complex subunits STAG2, RAD21, SMC3. This protein complex is important for sister chromatid cohesion, chromosome segregation, DNA repair, genome organization, and gene expression. The STAG2 subunit of the complex is highly mutated in bladder and myeloid cancers, and LOF mutations on STAG2 are correlated with DNA damage [52-54].

The sensitivity or responsivity of a drug action to a targeted cancer depends on how much the tumor relies on the particular oncogene and the cellular pathway with which it is associated. In PIK3CA, a combination of a driver mutation with either driver, weak driver, or strong latent driver, particularly under different mechanism of actions, have a good therapeutic response.

Conclusions

In conclusion, we developed a comprehensive approach to discover latent driver mutations. We integrated molecular profiles of more than 80K patient tumors, drug treatment data of cancer cell lines and PDXs from multiple sources to reveal associations between molecular alterations to discover latent co-occurring driver mutations in the same allele, in non-redundant pathways and metastatic patterns with the help of multiple informatics techniques and interpret them through their clinical impact. Our results, supported by drug response data of cell lines and patient-derived xenografts, and transcriptomic profiles of single and double mutant tumors, provide a strong background for therapeutic potentials of double mutations. We believe that the results of this study may form a basis for further experimental evaluation of molecular alterations to be exploited for therapeutic purposes across different cancer types. Mechanistically, the actions of *same gene* double mutations are more straightforward to interpret as compared to double mutations in different protein in independent pathways. How double mutations in independent pathways work is highly challenging to understand.

Figure Legends

Figure 1. Overall statistics of the data set, mutation load and double mutations, and analysis of the significant double mutations. **(A)** Total number of tumors, alterations, cancer types in the union of TCGA and AACR GENIE studies. Same gene double and different gene double mutations are found by the Mann-Whitney U test. Windrose plot showing the number of same gene double mutant (blue) tumors across 34 tissues (Oncotree) on the log-scale axis. Green portion represents the amount of tumors without any significant double mutation. **(B)** Tissue specificity of same gene dual mutations compared to their single mutant counterparts. X-axis shows the ratio of the number of tissues containing double and single mutant tumors in each gene. Y-axis shows the fraction of overall count of double mutant tumors to the single mutant ones. Smaller values along the x-axis indicates tissue specific same gene double mutations. Genes having cancer-specific double mutations are red and cancer-wide double mutations are in blue. **(C)** Composition of the double mutations based on known driver (D) and potential latent driver (d) labels in tumor suppressor genes and oncogenes where D is already known frequent driver mutations, d is relatively rare potential latent drivers. Fraction (%) of DD, Dd, dd type double mutations are significantly different between oncogenes and tumor suppressor genes. **(D)** Box plot showing passenger mutation load in tumor suppressor genes and oncogenes. The patient group carrying same gene double mutations on oncogenes have relatively smaller passenger mutation counts compared to the group carrying double mutation on tumor suppressor genes. **(E)** Tumor count distributions of known driver and potential latent driver mutations. Known driver mutations are observed more frequently that the potential latent driver mutations. **(F)** Grouped bar plot shows the fraction (%) of alterations in chemical properties of amino acids for oncogenes and tumor suppressor genes. Mutations on oncogenes mostly convert hydrophobic

525 residues to charged, and mutations on tumor suppressor genes usually convert charged residues
526 to polar.

527

528 **Figure 2.** Same gene double mutations are specific to some tissues or cancer subtypes. Bubble
529 plots show number (node size) and frequency (node color) of double-mutant tumors among
530 gene-mutant tumors across different tissues and cancer subtypes (Oncotree). For the 35 genes
531 with significant same gene double mutations, node size represents the number of patients
532 carrying at least one doublet on a gene in a tissue or cancer type. **(A)** Presence of same gene
533 double mutations across different cancer tissues where at least 3 tumors carry at least one same
534 gene double mutation on one of the 35 genes. **(B)** Presence of different gene dual mutations
535 across different cancer subtypes. The cancer subtypes where at least 5 tumors carry at least one
536 double mutation are listed on the y-axis. **(C)** Representation of mutations in genes to compose a
537 doublet as a circular diagram. Circumference of the circles divided into arcs proportional to the
538 frequency of each mutated residue. The strips from one residue to another represents significant
539 double mutations with size of strips indicating frequency of each double mutation.

540

541 **Figure 3.** A detailed analysis of PIK3CA double mutation profile, 3D structure and clinical
542 implications. **(A)** Paired dot plot of the 46 double mutations on PIK3CA, and the number of
543 tumors carrying them. Colors indicate type of a mutation, driver (purple), weak driver (orchid),
544 strong latent driver (blue), weak latent driver (light blue). Drivers and weak drivers are known
545 driver mutations with ≥500 and <500 harboring tumors respectively. Strong latent drivers and
546 weak latent drivers are potential latent driver mutations carried by ≥10 and <10 tumors
547 respectively. There are 3 *driver/driver*, 13 weak *driver/weak driver*, 5 *driver/strong latent driver,*

548 35 *driver/weak driver. P104, E726 and M1004 have a potential to be strong latent drivers.* **(B)**
549 Presence of PIK3CA same gene dual mutations across different cancer tissues. Dots are scaled
550 based on the number of tumor having double mutations, and color corresponds to the percentage
551 of double mutant tumors among single mutants. **(C)** 3D structure of PIK3CA (PDB: 4OVV) with
552 H1047, E726, E542, E545, R88, R93, P539. **(D)** Response of PIK3CA double mutant breast
553 cancer cell lines to drugs in network representation. BT-20 (H1047/P539) and CAL148
554 (H1047/D350) becomes sensitive to PI3K/MTOR pathway targeting drugs. **(E)** PIK3CA
555 mutation doublets in breast cancer and the associated violin plot illustrating response to PI3Kɣ
556 inhibitors. H1047/P539 double mutant tumor becomes more sensitive to PI3Kɣ inhibitors **(F)**
557 Tumor volume change of single and double PIK3CA mutant xenografts without any treatment.
558 There is a remarkable tumor increase in the double mutant xenograft. **(G)** Tumor volume
559 comparison of the single and double mutant xenografts without any treatment and with BYL719
560 (Alpelisib) treatment, the double mutant xenograft responds better to the PI3Kα inhibitor drug.
561 **(H)** Comparing tumor volume changes of the dual PIK3CA mutant xenografts without any
562 treatment and with BYL719 and BYL719+LJM716 treatment. The tumor growth of the double
563 mutant xenograft X-2524 is prominently slow when a combination therapy BYL719+LJM716 is
564 applied compared to untreated and BYL719 treatment alone.
565

566 **Figure 4.** Representation of double mutations in EGFR, BRAF, APC and PTEN. Each paired dot
567 represents one double mutation. Dots are colored according to their type, driver (purple), weak
568 driver (orchid), strong latent driver (blue), weak latent driver (sky blue). **(A)** Double mutations
569 and corresponding number of mutated tumors of each component reveals that there are 5
570 driver/driver, 5 weak driver/weak driver combinations and 1 weak driver/strong latent driver

combinations; V774 might be a strong latent driver**. (B)** Genes harboring 12 double mutations, 7 are different combinations of strong latent drivers E317, E319, I710, L711, I714, E715 and L721, and the rest are V600 (driver) composed of a double mutation with the strong latent drivers. **(C)** PTEN carries 15 double mutations with only one potential strong latent driver (N323)**. (D)** There are 25 double mutations on APC, R499, R564, E1408, S1465, T1487, T1556 that are potential strong latent drivers.

Figure 5. A wider analysis of double mutations in cell lines and association of doublets to drug response for clinical implications. **(A)** Prevalence of the double mutations in tissues associated with cell lines. APC, EGFR, NRAS double mutant cell lines belong to bowel, lung and ovarian tissues respectively. There are two cell lines in bowel tissue carrying PTEN double mutations, and five cell lines in lymph tissue with TP53 double mutations. **(B)** EGFR mutation doublets in lung cancer cell lines and their response to drugs in network representation. Among eight drugs targeting EGFR and RTK pathways, $EGFR^{L858/T790}$ mutant cell line is only sensitive to Pelitinib, and it is unresponsive to the rest, although the $EGFR^{L858}$ mutant cell line is sensitive to all. **(C)** Representation of dual mutations in EGFR structure. **(D)** EGFR mutation doublets in lung cancer together with the violin plot that shows the response to RTK inhibitor in dual mutant and single mutant cell lines. More negative z-score means more sensitivity and more positive z-score means more resistance to the drug molecule (**E)** PTEN and **(F)** APC mutation doublets in colon cancer cell lines and their response to drugs in network representation.

List of abbreviations

PDX – Patient-derived xenograft

TCGA – The Cancer Genome Atlas

GENIE – Genomics Evidence Neoplasia Information Exchange

PDB – Protein Databank

Declarations

Ethics approval and consent to participate.

Not applicable

Consent for publication

Not applicable

Availability of data and materials

The results shown here are in whole or part based upon data generated by the TCGA Research Network: https://www.cancer.gov/tcga. The authors would like to acknowledge the American Association for Cancer Research and its financial and material support in the development of the AACR Project GENIE registry, as well as members of the consortium for their commitment to data sharing. Interpretations are the responsibility of the study authors. The cell line data underlying the results presented in the study are available from GDSC in https://www.cancerrxgene.org/downloads, Cell Model Passports in https://cellmodelpassports.sanger.ac.uk/downloads, and The Cancer Dependency Map project in https://depmap.org/portal/download/. The PDX data underlying the results presented in the study are available in Gao et al [38].

Competing interests

The authors declare that they have no competing interests.

Funding

This project has been funded in whole or in part with federal funds from the National Cancer Institute, National Institutes of Health, under contract HHSN261200800001E. The content of this publication does not necessarily reflect the views or policies of the Department of Health and Human Services, nor does mention of trade names, commercial products or organizations imply endorsement by the US Government. This Research was supported [in part] by the Intramural Research Program of the NIH, National Cancer Institute, Center for Cancer Research and the Intramural Research Program of the NIH Clinical Center. NT has received support from the Career Development Program of TUBITAK under the project number 117E192, UNESCO-L'Oreal National for Women in Science Fellowship and UNESCO-L'Oréal International Rising Talent Fellowship and TUBA-GEBIP.

Authors' contributions

Conceptualization: CJT, RN, NT

Data curation: BRY

Formal analysis: BRY, CJT, NT

Methodology: BRY, CJT, RN, NT

Project administration: NT

Supervision: NT

Visualization: BRY, NT

Writing – original draft: BRY, CJT, RN, NT

Writing – review and editing: BRY, CJT, RN, NT

References

1. Vogelstein B, Papadopoulos N, Velculescu VE, Zhou S, Diaz LA, Kinzler KW: **Cancer genome landscapes**. *science* 2013, **339**(6127):1546-1558.
2. McFarland CD, Korolev KS, Kryukov GV, Sunyaev SR, Mirny LA: **Impact of deleterious passenger mutations on cancer progression**. *Proceedings of the National Academy of Sciences* 2013, **110**(8):2910-2915.
3. Kotler E, Shani O, Goldfeld G, Lotan-Pompan M, Tarcic O, Gershoni A, Hopf TA, Marks DS, Oren M, Segal E: **A systematic p53 mutation library links differential functional impact to cancer mutation pattern and evolutionary conservation**. *Molecular cell* 2018, **71**(1):178-190. e178.
4. McFarland CD, Yaglom JA, Wojtkowiak JW, Scott JG, Morse DL, Sherman MY, Mirny LA: **The damaging effect of passenger mutations on cancer progression**. *Cancer research* 2017, **77**(18):4763-4772.
5. Nussinov R, Jang H, Tsai C-J, Cheng F: **Precision medicine review: rare driver mutations and their biophysical classification**. *Biophysical reviews* 2019, **11**(1):5-19.
6. Nussinov R, Tsai C-J: **'Latent drivers' expand the cancer mutational landscape**. *Current Opinion in Structural Biology* 2015, **32**:25-32.
7. Castro-Giner F, Ratcliffe P, Tomlinson I: **The mini-driver model of polygenic cancer evolution**. *Nature Reviews Cancer* 2015, **15**(11):680-685.

8. Sondka Z, Bamford S, Cole CG, Ward SA, Dunham I, Forbes SA: **The COSMIC Cancer Gene Census: describing genetic dysfunction across all human cancers**. *Nature Reviews Cancer* 2018, **18**(11):696-705.

9. An O, Dall'Olio GM, Mourikis TP, Ciccarelli FD: **NCG 5.0: updates of a manually curated repository of cancer genes and associated properties from cancer mutational screenings**. *Nucleic acids research* 2016, **44**(D1):D992-D999.

10. Tamborero D, Rubio-Perez C, Deu-Pons J, Schroeder MP, Vivancos A, Rovira A, Tusquets I, Albanell J, Rodon J, Tabernero J: **Cancer Genome Interpreter annotates the biological and clinical relevance of tumor alterations**. *Genome medicine* 2018, **10**(1):25.

11. Mularoni L, Sabarinathan R, Deu-Pons J, Gonzalez-Perez A, López-Bigas N: **OncodriveFML: a general framework to identify coding and non-coding regions with cancer driver mutations**. *Genome biology* 2016, **17**(1):1-13.

12. Arnedo-Pac C, Mularoni L, Muiños F, Gonzalez-Perez A, Lopez-Bigas N: **OncodriveCLUSTL: a sequence-based clustering method to identify cancer drivers**. *Bioinformatics* 2019, **35**(22):4788-4790.

13. Gundem G, Perez-Llamas C, Jene-Sanz A, Kedzierska A, Islam A, Deu-Pons J, Furney SJ, Lopez-Bigas N: **IntOGen: integration and data mining of multidimensional oncogenomic data**. *Nature methods* 2010, **7**(2):92-93.

14. Martínez-Jiménez F, Muiños F, Sentís I, Deu-Pons J, Reyes-Salazar I, Arnedo-Pac C, Mularoni L, Pich O, Bonet J, Kranas H: **A compendium of mutational cancer driver genes**. *Nature Reviews Cancer* 2020, **20**(10):555-572.

15. Bailey MH, Tokheim C, Porta-Pardo E, Sengupta S, Bertrand D, Weerasinghe A, Colaprico A, Wendl MC, Kim J, Reardon B: **Comprehensive characterization of cancer driver genes and mutations**. *Cell* 2018, **173**(2):371-385. e318.

16. Ramos AH, Lichtenstein L, Gupta M, Lawrence MS, Pugh TJ, Saksena G, Meyerson M, Getz G: **Oncotator: cancer variant annotation tool**. *Human mutation* 2015, **36**(4):E2423-E2429.

17. Chen S, He X, Li R, Duan X, Niu B: **HotSpot3D web server: an integrated resource for mutation analysis in protein 3D structures**. *Bioinformatics* 2020.

18. Niu B, Scott AD, Sengupta S, Bailey MH, Batra P, Ning J, Wyczalkowski MA, Liang W-W, Zhang Q, McLellan MD: **Protein-structure-guided discovery of functional mutations across 19 cancer types**. *Nature genetics* 2016, **48**(8):827-837.

19. Dincer C, Kaya T, Keskin O, Gursoy A, Tuncbag N: **3D spatial organization and network-guided comparison of mutation profiles in Glioblastoma reveals similarities across patients**. *PLoS computational biology* 2019, **15**(9):e1006789.

20. Evans P, Avey S, Kong Y, Krauthammer M: **Adjusting for background mutation frequency biases improves the identification of cancer driver genes**. *IEEE transactions on nanobioscience* 2013, **12**(3):150-157.

21. Nussinov R, Tsai C-J, Jang H: **Why are some driver mutations rare?** *Trends in pharmacological sciences* 2019, **40**(12):919-929.

22. Donehower LA, Soussi T, Korkut A, Liu Y, Schultz A, Cardenas M, Li X, Babur O, Hsu T-K, Lichtarge O: **Integrated analysis of TP53 gene and pathway alterations in the cancer genome atlas**. *Cell reports* 2019, **28**(5):1370-1384. e1375.

23. Bozic I, Antal T, Ohtsuki H, Carter H, Kim D, Chen S, Karchin R, Kinzler KW, Vogelstein B, Nowak MA: **Accumulation of driver and passenger mutations during tumor progression**. *Proceedings of the National Academy of Sciences* 2010, **107**(43):18545-18550.

24. Risques RA, Kennedy SR: **Aging and the rise of somatic cancer-associated mutations in normal tissues**. *PLoS genetics* 2018, **14**(1):e1007108.

25. Vasan N, Razavi P, Johnson JL, Shao H, Shah H, Antoine A, Ladewig E, Gorelick A, Lin T-Y, Toska E: **Double PIK3CA mutations in cis increase oncogenicity and sensitivity to PI3Kα inhibitors**. *Science* 2019, **366**(6466):714-723.

26. Gorelick AN, Sánchez-Rivera FJ, Cai Y, Bielski CM, Biederstedt E, Jonsson P, Richards AL, Vasan N, Penson AV, Friedman ND: **Phase and context shape the function of composite oncogenic mutations**. *Nature* 2020:1-4.

27. Saito Y, Koya J, Araki M, Kogure Y, Shingaki S, Tabata M, McClure MB, Yoshifuji K, Matsumoto S, Isaka Y: **Landscape and function of multiple mutations within individual oncogenes**. *Nature* 2020:1-5.

28. Raimondi F, Inoue A, Kadji FM, Shuai N, Gonzalez J-C, Singh G, de la Vega AA, Sotillo R, Fischer B, Aoki J: **Rare, functional, somatic variants in gene families linked to cancer genes: GPCR signaling as a paradigm**. *Oncogene* 2019, **38**(38):6491-6506.

29. Lehner B: **Molecular mechanisms of epistasis within and between genes**. *Trends in Genetics* 2011, **27**(8):323-331.

30. van de Haar J, Canisius S, Michael KY, Voest EE, Wessels LF, Ideker T: **Identifying epistasis in cancer genomes: a delicate affair**. *Cell* 2019, **177**(6):1375-1383.

720 31. Liu J, Lichtenberg T, Hoadley K, Poisson L, Lazar A, Cherniack A, Kovatich A, Benz C,
721 Levine D, Lee A: **Cancer Genome Atlas Research. 2018**. *An integrated TCGA pan-*
722 *cancer clinical data resource to drive high-quality survival outcome analytics Cell*,
723 **173**:400-416.
724 32. Consortium APG: **AACR Project GENIE: powering precision medicine through an**
725 **international consortium**. *Cancer discovery* 2017, **7**(8):818-831.
726 33. Cerami E, Gao J, Dogrusoz U, Gross BE, Sumer SO, Aksoy BA, Jacobsen A, Byrne CJ,
727 Heuer ML, Larsson E: **The cBio cancer genomics portal: an open platform for**
728 **exploring multidimensional cancer genomics data**. In.: AACR; 2012.
729 34. Goel MK, Khanna P, Kishore J: **Understanding survival analysis: Kaplan-Meier**
730 **estimate**. *International journal of Ayurveda research* 2010, **1**(4):274.
731 35. Gu Z, Eils R, Schlesner M: **Complex heatmaps reveal patterns and correlations in**
732 **multidimensional genomic data**. *Bioinformatics* 2016, **32**(18):2847-2849.
733 36. van der Meer D, Barthorpe S, Yang W, Lightfoot H, Hall C, Gilbert J, Francies HE,
734 Garnett MJ: **Cell Model Passports—a hub for clinical, genetic and functional datasets**
735 **of preclinical cancer models**. *Nucleic acids research* 2019, **47**(D1):D923-D929.
736 37. Yang W, Soares J, Greninger P, Edelman EJ, Lightfoot H, Forbes S, Bindal N, Beare D,
737 Smith JA, Thompson IR: **Genomics of Drug Sensitivity in Cancer (GDSC): a resource**
738 **for therapeutic biomarker discovery in cancer cells**. *Nucleic acids research* 2012,
739 **41**(D1):D955-D961.
740 38. Gao H, Korn JM, Ferretti S, Monahan JE, Wang Y, Singh M, Zhang C, Schnell C, Yang
741 G, Zhang Y: **High-throughput screening using patient-derived tumor xenografts to**
742 **predict clinical trial drug response**. *Nature medicine* 2015, **21**(11):1318-1325.

39. Chen Z, Feng J, Saldivar J, Gu D, Bockholt A, Sommer S: **EGFR somatic doublets in lung cancer are frequent and generally arise from a pair of driver mutations uncommonly seen as singlet mutations: one-third of doublets occur at five pairs of amino acids**. *Oncogene* 2008, **27**(31):4336-4343.

40. Gao J, Chang MT, Johnsen HC, Gao SP, Sylvester BE, Sumer SO, Zhang H, Solit DB, Taylor BS, Schultz N: **3D clusters of somatic mutations in cancer reveal numerous rare mutations as functional targets**. *Genome medicine* 2017, **9**(1):4.

41. Xu X, Zhao J, Xu Z, Peng B, Huang Q, Arnold E, Ding J: **Structures of human cytosolic NADP-dependent isocitrate dehydrogenase reveal a novel self-regulatory mechanism of activity**. *Journal of Biological Chemistry* 2004, **279**(32):33946-33957.

42. Hobbs GA, Der CJ: **RAS mutations are not created equal**. *Cancer discovery* 2019, **9**(6):696-698.

43. Poulin EJ, Bera AK, Lu J, Lin Y-J, Strasser SD, Paulo JA, Huang TQ, Morales C, Yan W, Cook J: **Tissue-specific oncogenic activity of KRASA146T**. *Cancer discovery* 2019, **9**(6):738-755.

44. Chin CV, Antony J, Ketharnathan S, Labudina A, Gimenez G, Parsons KM, He J, George AJ, Pallota MM, Musio A: **Cohesin mutations are synthetic lethal with stimulation of WNT signaling**. *Elife* 2020, **9**:e61405.

45. Zhang M, Jang H, Nussinov R: **PI3K Driver Mutations: A Biophysical Membrane-Centric Perspective**. *Cancer Research* 2020.

46. Zhang M, Jang H, Nussinov R: **Structural Features that Distinguish Inactive and Active PI3K Lipid Kinases**. *Journal of molecular biology* 2020, **432**(22):5849-5859.

765 47. Zhang M, Jang H, Nussinov R: **The structural basis for Ras activation of PI3Kα lipid**
766 **kinase**. *Physical Chemistry Chemical Physics* 2019, **21**(22):12021-12028.
767 48. Rodrigues CH, Pires DE, Ascher DB: **DynaMut: predicting the impact of mutations**
768 **on protein conformation, flexibility and stability**. *Nucleic acids research* 2018,
769 **46**(W1):W350-W355.
770 49. Liu X, Lu S, Song K, Shen Q, Ni D, Li Q, He X, Zhang H, Wang Q, Chen Y:
771 **Unraveling allosteric landscapes of allosterome with ASD**. *Nucleic acids research*
772 2020, **48**(D1):D394-D401.
773 50. Shannon P, Markiel A, Ozier O, Baliga NS, Wang JT, Ramage D, Amin N, Schwikowski
774 B, Ideker T: **Cytoscape: a software environment for integrated models of**
775 **biomolecular interaction networks**. *Genome research* 2003, **13**(11):2498-2504.
776 51. Yao Z, Yaeger R, Rodrik-Outmezguine VS, Tao A, Torres NM, Chang MT, Drosten M,
777 Zhao H, Cecchi F, Hembrough T: **Tumours with class 3 BRAF mutants are sensitive**
778 **to the inhibition of activated RAS**. *Nature* 2017, **548**(7666):234-238.
779 52. Romero-Pérez L, Surdez D, Brunet E, Delattre O, Grünewald TG: **STAG mutations in**
780 **cancer**. *Trends in Cancer* 2019, **5**(8):506-520.
781 53. Hill VK, Kim J-S, Waldman T: **Cohesin mutations in human cancer**. *Biochimica et*
782 *Biophysica Acta (BBA)-Reviews on Cancer* 2016, **1866**(1):1-11.
783 54. Ding S, Diep J, Feng N, Ren L, Li B, Ooi YS, Wang X, Brulois KF, Yasukawa LL, Li X:
784 **STAG2 deficiency induces interferon responses via cGAS-STING pathway and**
785 **restricts virus infection**. *Nature communications* 2018, **9**(1):1-8.

786

A

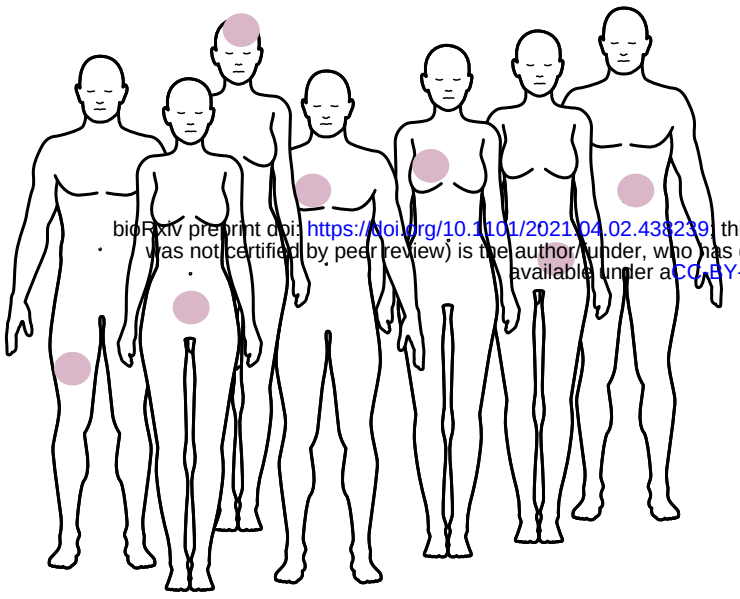

78837 Tumor Samples
671 Cancer Types, 34 Tissues
1638191 Alterations

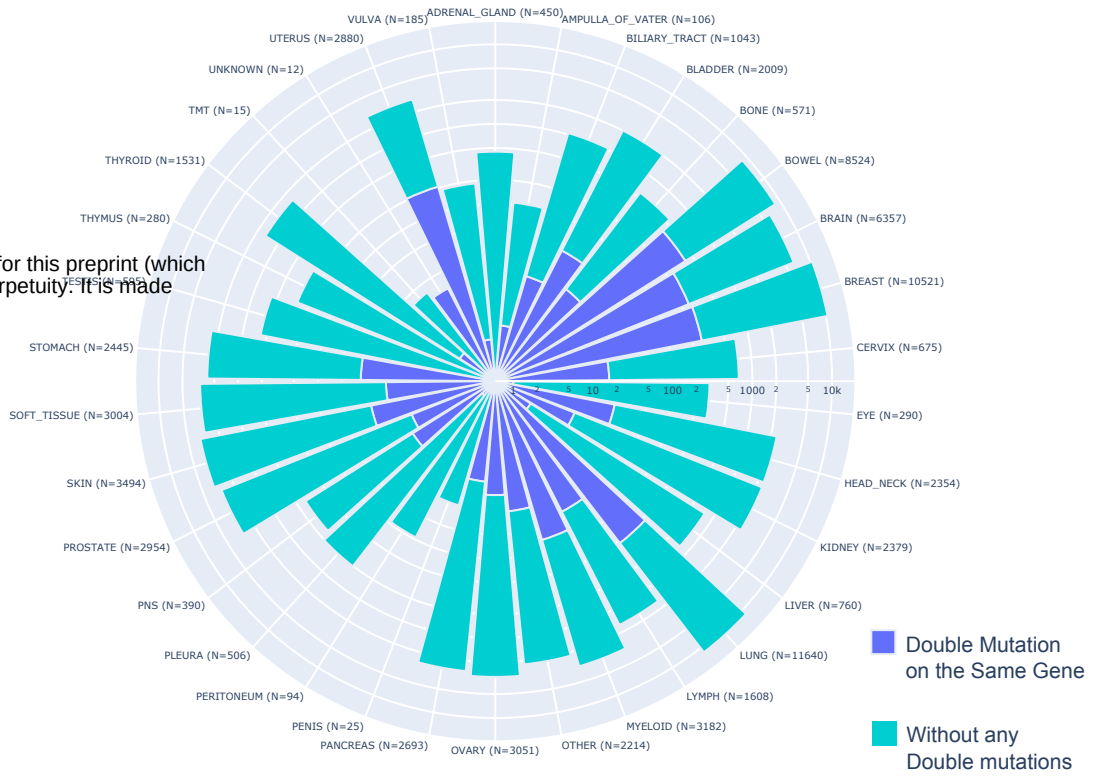

B

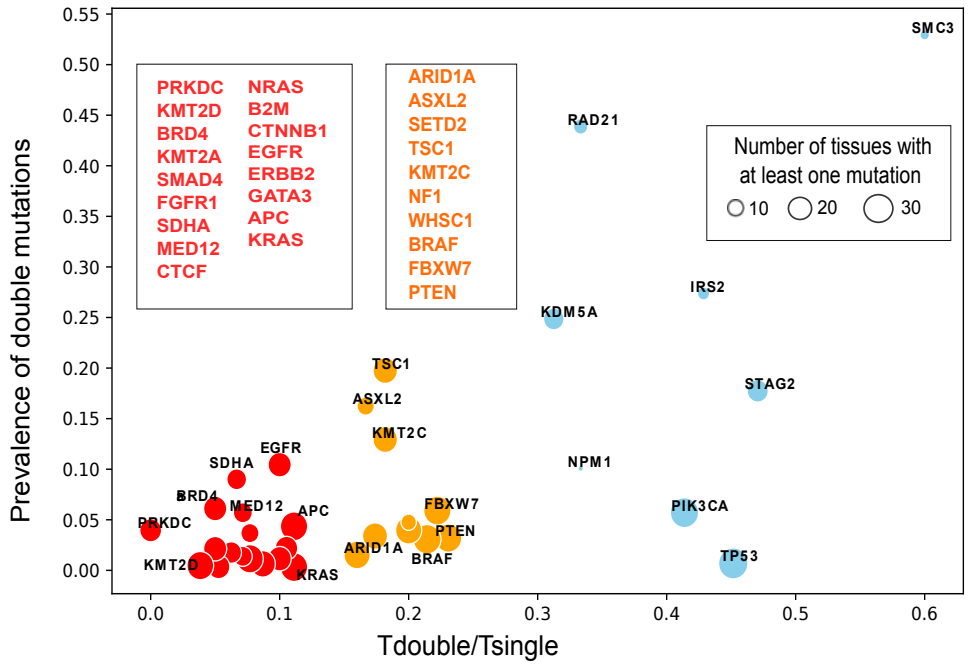

C

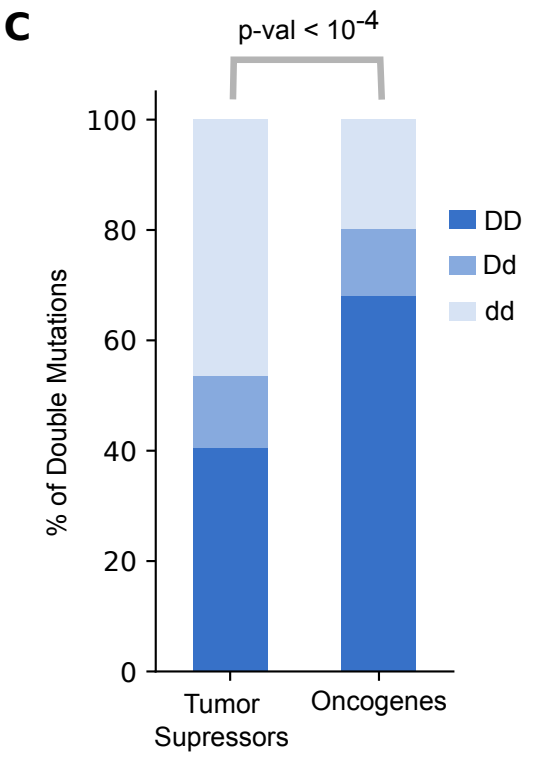

D

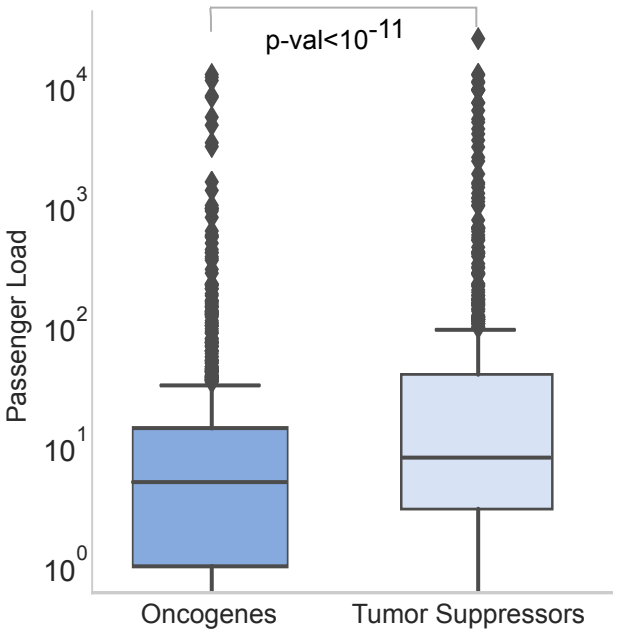

E

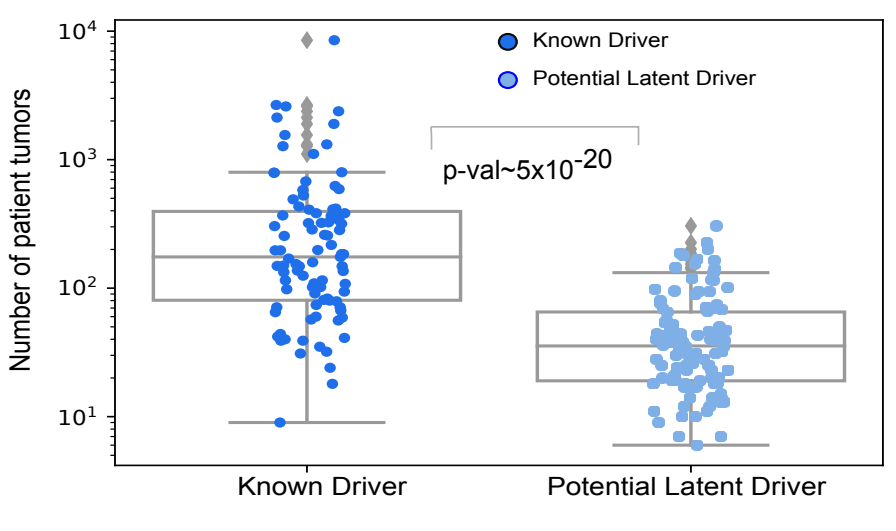

F

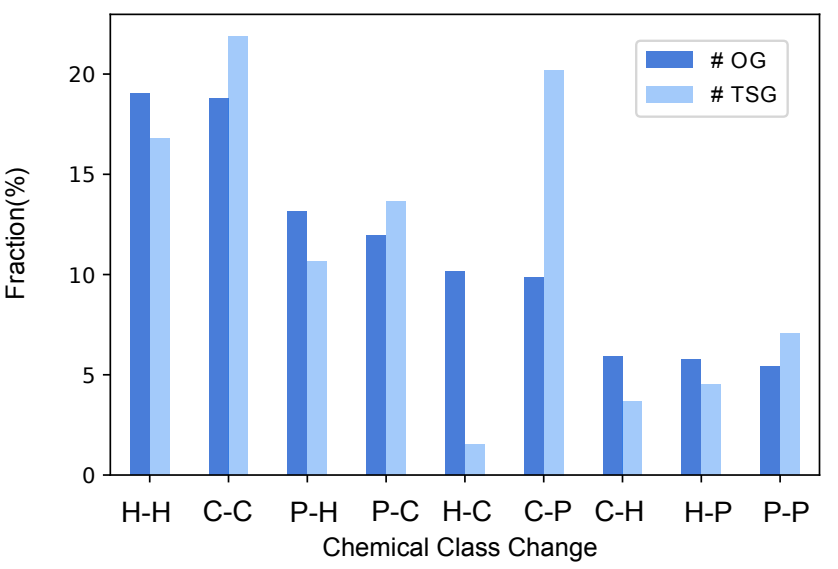

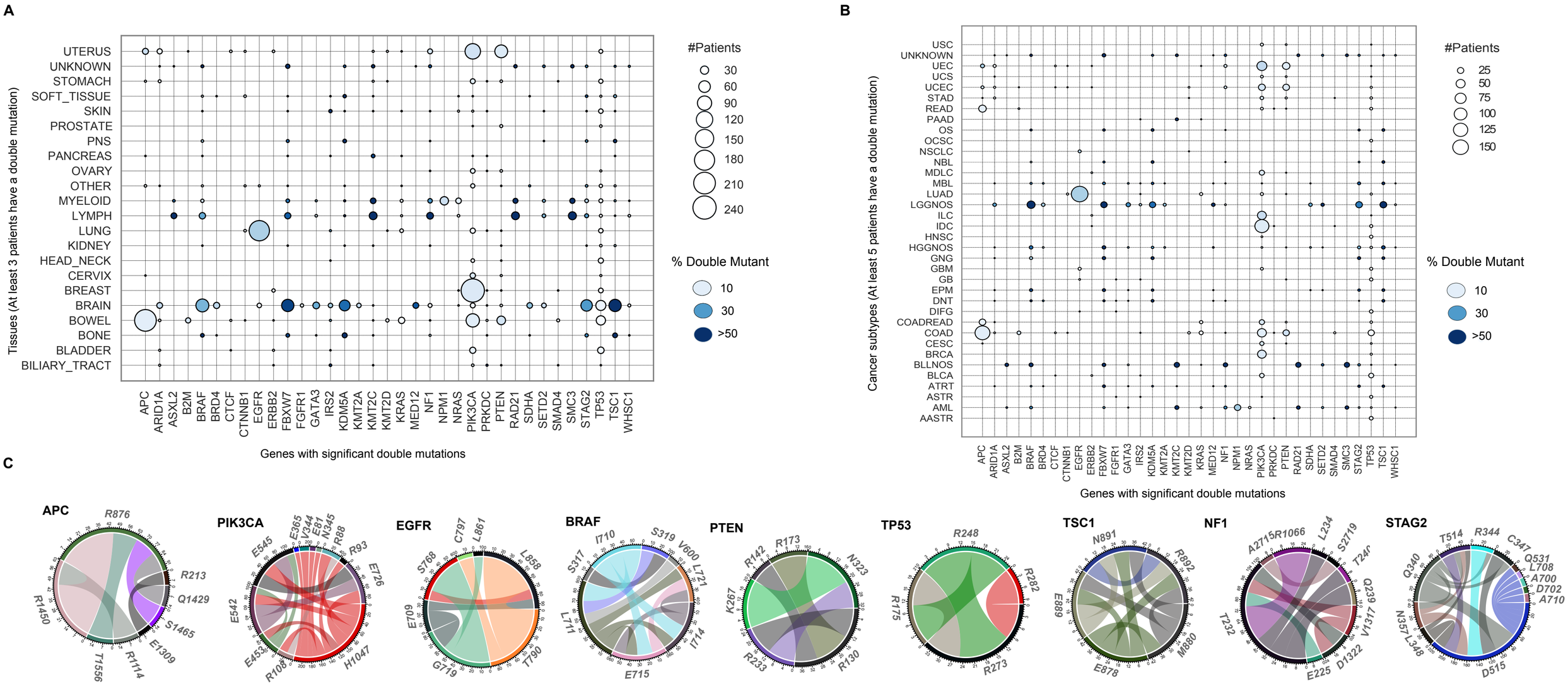
A
Tissues (At least 3 patients have a double mutation)
UTERUS
UNKNOWN
STOMACH
SOFT_TISSUE
SKIN
PROSTATE
PNS
PANCREAS
OVARY
OTHER
MYELOID
LYMPH
LUNG
KIDNEY
HEAD_NECK
CERVIX
BREAST
BRAIN
BOWEL
BONE
BLADDER
BILIARY_TRACT
APC ARID1A ASXL2 B2M BRAF BRD4 CTCF CTNNB1 EGFR ERBB2 FBXW7 FGFR1 GATA3 IRS2 KDM5A KMT2A KMT2C KMT2D KRAS MED12 NF1 NPM1 NRAS PIK3CA PRKDC PTEN RAD21 SDHA SETD2 SMAD4 SMC3 STAG2 TP53 TSC1 WHSC1
Genes with significant double mutations
#Patients
30
60
90
120
150
180
210
240
% Double Mutant
10
30
>50
B
Cancer subtypes (At least 5 patients have a double mutation)
USC
UNKNOWN
UEC
UCS
UCEC
STAD
READ
PAAD
OS
OCSC
NSCLC
NBL
MDLC
MBL
LUAD
LGGNOS
ILC
IDC
HNSC
HGGNOS
GNG
GBM
GB
EPM
DNT
DIFG
COADREAD
COAD
CESC
BRCA
BLLNOS
BLCA
ATRT
ASTR
AML
AASTR
APC ARID1A ASXL2 B2M BRAF BRD4 CTCF CTNNB1 EGFR ERBB2 FBXW7 FGFR1 GATA3 IRS2 KDM5A KMT2A KMT2C KMT2D KRAS MED12 NF1 NPM1 NRAS PIK3CA PRKDC PTEN RAD21 SDHA SETD2 SMAD4 SMC3 STAG2 TP53 TSC1 WHSC1
Genes with significant double mutations
#Patients
25
50
75
100
125
150
% Double Mutant
10
30
>50
C
APC
R876
R213
Q1429
S1465
E1309
R1114
T1556
R1450
PIK3CA
E365
V344
E81
N345
R88
R93
E726
H1047
T790
G719
R108
E453
E542
E545
EGFR
C797
L861
L858
T790
E709
S768
BRAF
I710
S319
V600
L721
I714
E715
L711
S317
PTEN
R142
R173
N323
R130
R233
K267
TP53
R248
R282
R273
R175
TSC1
N891
R892
M880
E878
E889
NF1
A2715R1066
L234
S2719
T24
Q2339
V1317
D1322
E225
T232
STAG2
T514
R344
C347
Q531
L708
A700
D702
A710
D515
N357
L348
Q340

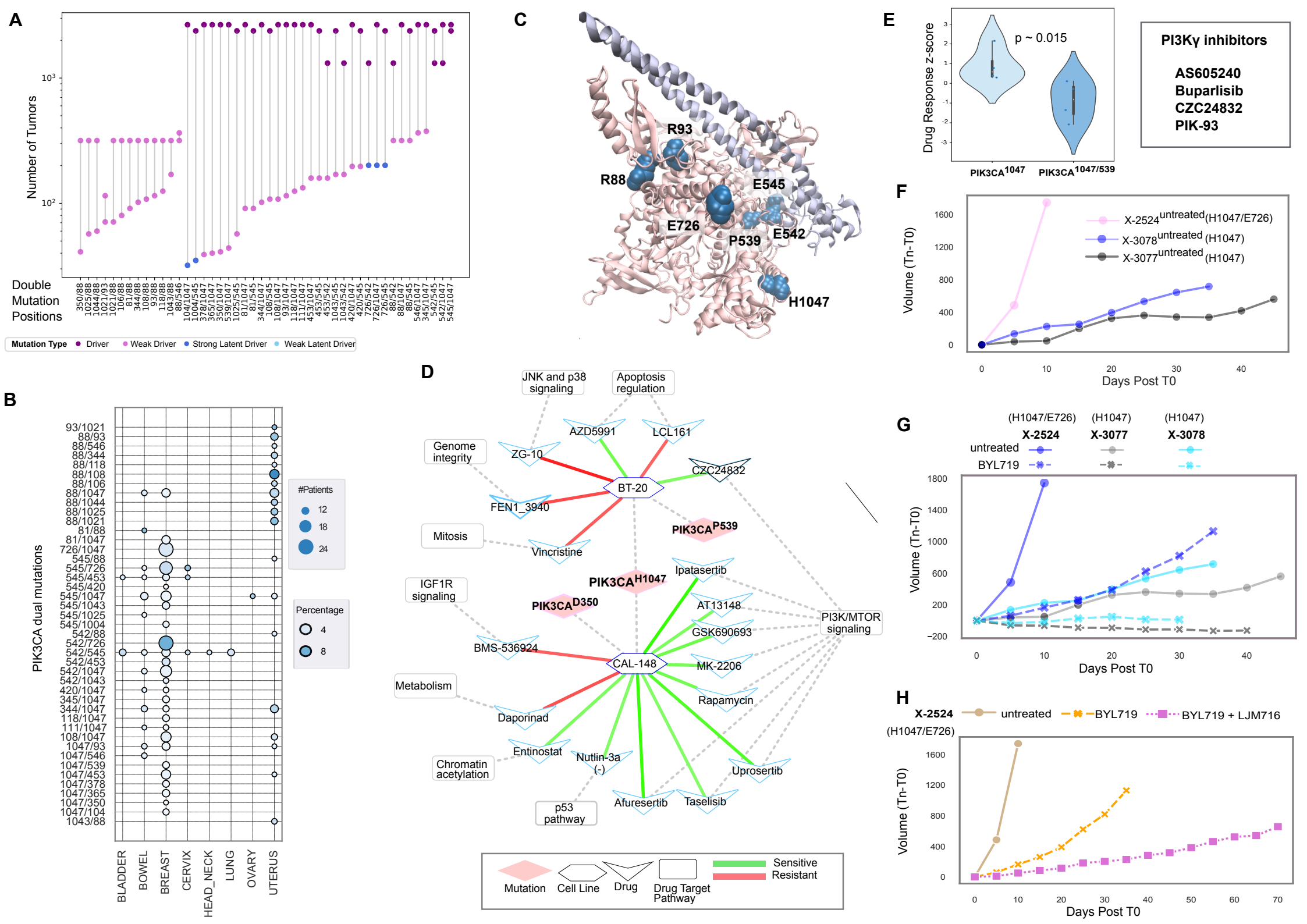
A
Number of Tumors
Double Mutation Positions
Mutation Type
Driver
Weak Driver
Strong Latent Driver
Weak Latent Driver
B
PIK3CA dual mutations
#Patients
Percentage
BLADDER
BOWEL
BREAST
CERVIX
HEAD_NECK
LUNG
OVARY
UTERUS
C
R93
R88
E545
E726
P539
E542
H1047
D
JNK and p38 signaling
Apoptosis regulation
Genome integrity
Mitosis
IGF1R signaling
Metabolism
Chromatin acetylation
p53 pathway
PI3K/MTOR signaling
AZD5991
LCL161
ZG-10
CZC24832
FEN1_3940
Vincristine
Ipatasertib
AT13148
GSK690693
MK-2206
Rapamycin
Uprosertib
Taselisib
Afuresertib
Entinostat
Nutlin-3a (-)
Daporinad
BMS-536924
BT-20
CAL-148
PIK3CA P539
PIK3CA H1047
PIK3CA D350
Mutation
Cell Line
Drug
Drug Target Pathway
Sensitive
Resistant
E
Drug Response z-score
p ~ 0.015
PIK3CA 1047
PIK3CA 1047/539
PI3Kγ inhibitors
AS605240
Buparlisib
CZC24832
PIK-93
F
Volume (Tn-T0)
Days Post T0
X-2524 untreated (H1047/E726)
X-3078 untreated (H1047)
X-3077 untreated (H1047)
G
(H1047/E726)
(H1047)
(H1047)
X-2524
X-3077
X-3078
untreated
BYL719
Volume (Tn-T0)
Days Post T0
H
X-2524
untreated
BYL719
BYL719 + LJM716
(H1047/E726)
Volume (Tn-T0)
Days Post T0

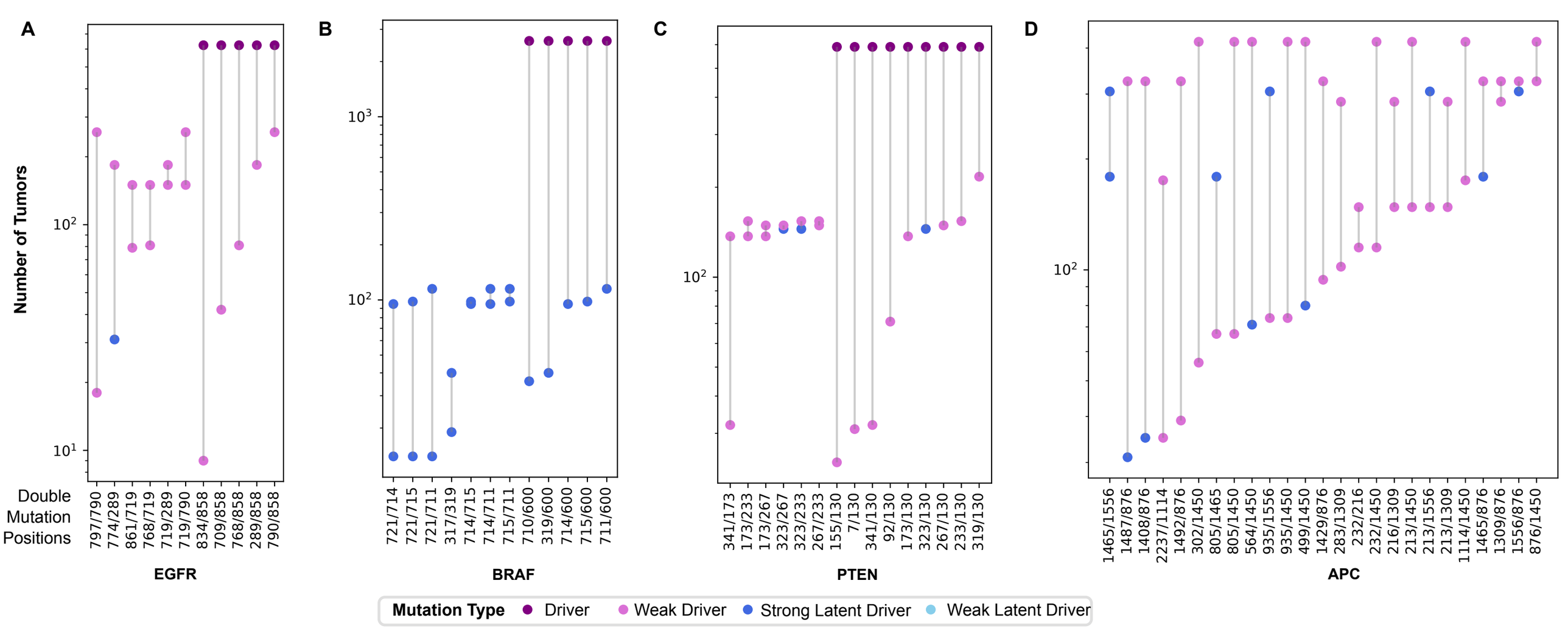
A
B
C
D
Number of Tumors
10^2
10^1
10^3
Double Mutation Positions
797/790
774/289
861/719
768/719
719/289
719/790
834/858
709/858
768/858
289/858
790/858
EGFR
721/714
721/715
721/711
317/319
714/715
714/711
715/711
710/600
319/600
714/600
715/600
711/600
BRAF
341/173
173/233
173/267
323/267
323/233
267/233
155/130
7/130
341/130
92/130
173/130
323/130
267/130
233/130
319/130
PTEN
1465/1556
1487/876
1408/876
2237/1114
1492/876
302/1450
805/1465
805/1450
564/1450
935/1556
935/1450
499/1450
1429/876
283/1309
232/216
232/1450
216/1309
213/1450
213/1556
213/1309
1114/1450
1465/876
1309/876
1556/876
876/1450
APC
Mutation Type
Driver
Weak Driver
Strong Latent Driver
Weak Latent Driver

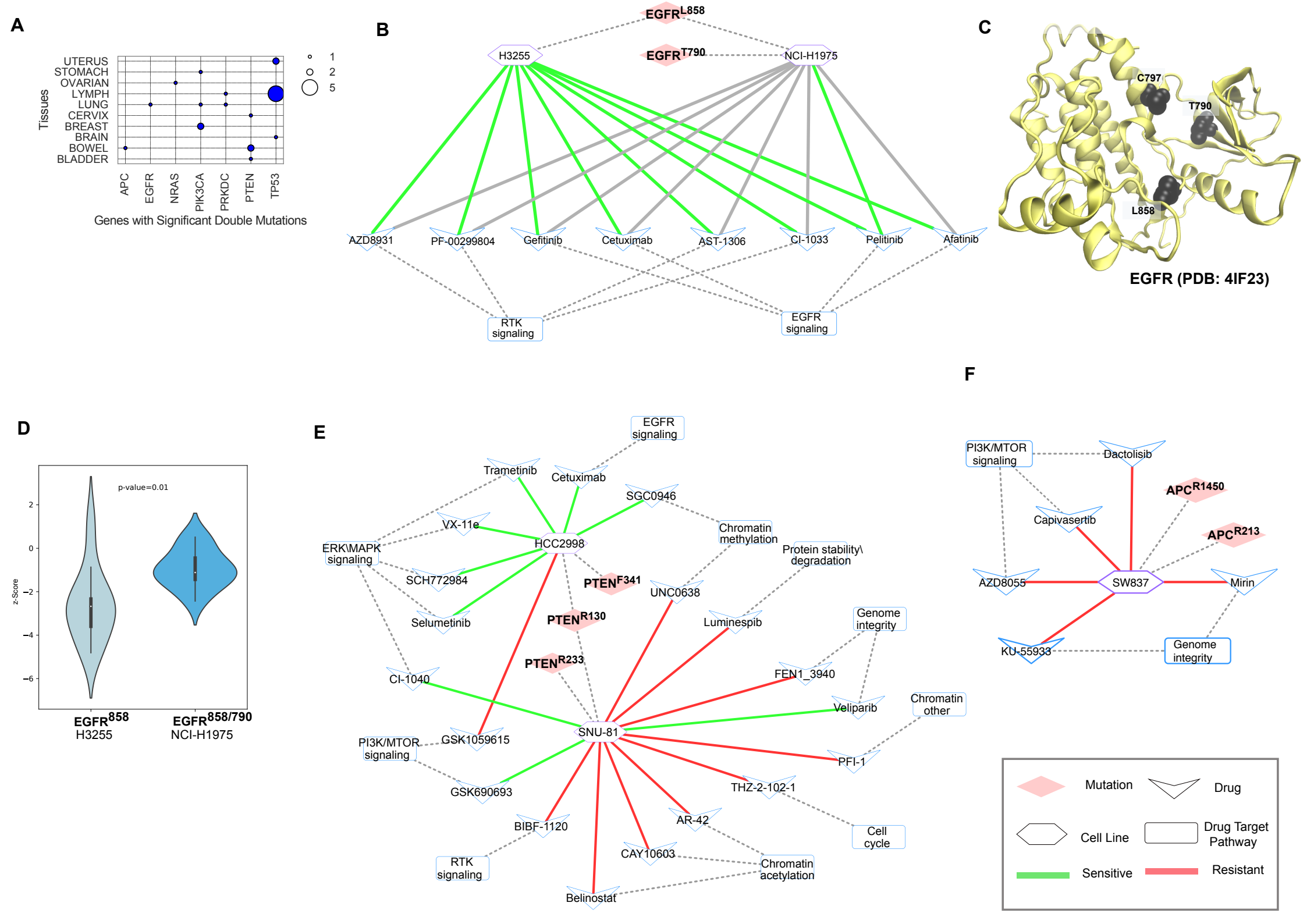
A
UTERUS
STOMACH
OVARIAN
LYMPH
LUNG
CERVIX
BREAST
BRAIN
BOWEL
BLADDER
Tissues
1
2
5
APC
EGFR
NRAS
PIK3CA
PRKDC
PTEN
TP53
Genes with Significant Double Mutations
B
EGFR L858
EGFR T790
H3255
NCI-H1975
AZD8931
PF-00299804
Gefitinib
Cetuximab
AST-1306
CI-1033
Pelitinib
Afatinib
RTK signaling
EGFR signaling
C
C797
T790
L858
EGFR (PDB: 4IF23)
D
p-value=0.01
z-Score
2
0
−2
−4
−6
EGFR 858
H3255
EGFR 858/790
NCI-H1975
E
EGFR signaling
Trametinib
Cetuximab
SGC0946
VX-11e
Chromatin methylation
Protein stability\ degradation
ERK\MAPK signaling
HCC2998
SCH772984
PTEN F341
UNC0638
Selumetinib
PTEN R130
Luminespib
Genome integrity
PTEN R233
CI-1040
FEN1_3940
Veliparib
Chromatin other
SNU-81
PI3K/MTOR signaling
GSK1059615
PFI-1
GSK690693
THZ-2-102-1
BIBF-1120
AR-42
Cell cycle
RTK signaling
CAY10603
Chromatin acetylation
Belinostat
F
PI3K/MTOR signaling
Dactolisib
APC R1450
Capivasertib
APC R213
AZD8055
SW837
Mirin
KU-55933
Genome integrity
Mutation
Drug
Cell Line
Drug Target Pathway
Sensitive
Resistant

Supplementary Text

Annotation of Double Mutations

We used domain and gene ontology (GO) information from InterPro, a consortium database collecting information from member databases, to annotate same gene double mutations (https://www.ebi.ac.uk/interpro/). Therefore a mutation position may match with more than one InterPro id, when this is the case we preferred Pfam annotation. If a mutation does not match with any Interpro id, we labelled it as "No_Domain_Info". We mapped the Interpro ID's to GO Annotations related to biological process, molecular function and cellular component categories. Usually an Interpro ID matches with more than one GO annotation. We constructed binary combinations of these domains for each component of a double mutation and counted the double mutations related to domain annotation combinations (similar procedure was conducted for GO annotations).

To find out spatial closeness of same gene double mutations we use 3DHotspots [1] which identifies statistically significant mutations clustering in 3D protein structures. There are 943 clusters of 504 different genes. If two mutated residues that are containing a dual mutation belong to the same cluster, we consider this same gene dual mutation components are in close proximity. We used Interactome Insider to identify if the components of either same gene or different gene double are located in the same interface [2]. Besides the experimental data in PDB and predicted data in Interactome3D, it also contains the predicted interfaces with their in-house method. We used EnrichR to find the pathway annotation of the genes having co-occurring mutations [3].

We matched the sequence position of each component of the same gene doublets to their InterPro domain, if available [4]. As a result, we mapped 113 out of 228 doublets to at least one Interpro domain. In case of more than one matching domain, we picked the Pfam original one, if available. Among them, only one component has domain information for 22 double mutations. In 96 doublets, both components have no domain information. We obtained a total of 19 InterPro domains. Mutations without any domain information are labeled 'No_Domain_Info' (this label covers cases whether the mutation position does not match with any domain or it belongs to loop, hinge regions). As shown in Figure S1A, a large portion of the mutations is in a region with domain annotation. Both components of 56 dual mutations are in the same domain. Doublets with domain information are either located in flexible or hinge or disordered regions or located in different domains.

A similar approach is applied to find GO molecular function information for partner mutations of doublets (Figure S1B). Both components of 57 dual mutations match with at least one GO molecular function annotation. Neither component of 151 dual mutations matches any GO Annotation. In the remaining 20 dual mutations, only one component matches with a GO annotation. Protein kinase activity and ATP binding are two molecular functions that are the most frequent annotations covering ~15% of the same gene dual mutations having GO annotation.

Alterations in Chemical Properties of amino acids

In order to classify alterations with respect to chemical classes of amino acids before and after mutations, we prepared a file containing unique rows as follows "patient barcode| gene | residue number | AA before mutation | AA after mutation". We excluded the cases where the final

amino acid is a stop codon. We calculated the fraction of chemical alterations on 2189 oncogene and 2262 tumor suppressor alterations among all oncogene and tumor suppressor alterations respectively (determined with respect to mutation positions). The 9 categories we evaluated in our analysis are Polar-Hydrophobic, Charged-Polar, Hydrophobic-Hydrophobic, Hydrophobic-Polar, Hydrophobic-Charged, Polar-Charged, Polar-Polar, Charged-Hydrophobic, Charged-Charged.

PIK3CA Stability Analysis via Dynamut Tool

Using the inactive state (PDB id: 4OVV) we calculated the folding free energy (ΔΔG) upon mutation using DynaMut [5] to assess the impact of single and double mutations on PIK3CA stability. Unsurprisingly, considering their diverse mechanism of action no clear trend is observed (Figure S8). For example, H1047R is a strong driver that promotes interaction with the membrane. It destabilization impact is minor (ΔΔG ≈ -0.5 kcal/mol). The impact of weak drivers R88Q and R93W is somewhat stronger (ΔΔG ≈ -1.5 kcal/mol and ΔΔG ≈ -1 kcal/mol, respectively). The effect of allosteric mutation D539R is also minor (ΔΔG ≈ -0.6 kcal/mol). Another strong driver E542K (ΔΔG ≈ 0.7 kcal/mol), stabilizes the protein like the weak drivers D350G (ΔΔG ≈ 0.5 kcal/mol) and E453Q (ΔΔG ≈ 0.3 kcal/mol). The most prominent stability changes occur when the strong driver H1047R cooperates with the allosteric mutation P539R (ΔΔG ≈ -2.3 kcal/mol) and the minor mutation P104L (ΔΔG ≈ -2.5 kcal/mol). These two dual mutations H1047R/P539R and H1047R/P104L destabilize the protein as do T1025A/R88Q (ΔΔG ≈ 0.7 kcal/mol) while T1025A and R88Q have a destabilizing effect.

Supplementary figures

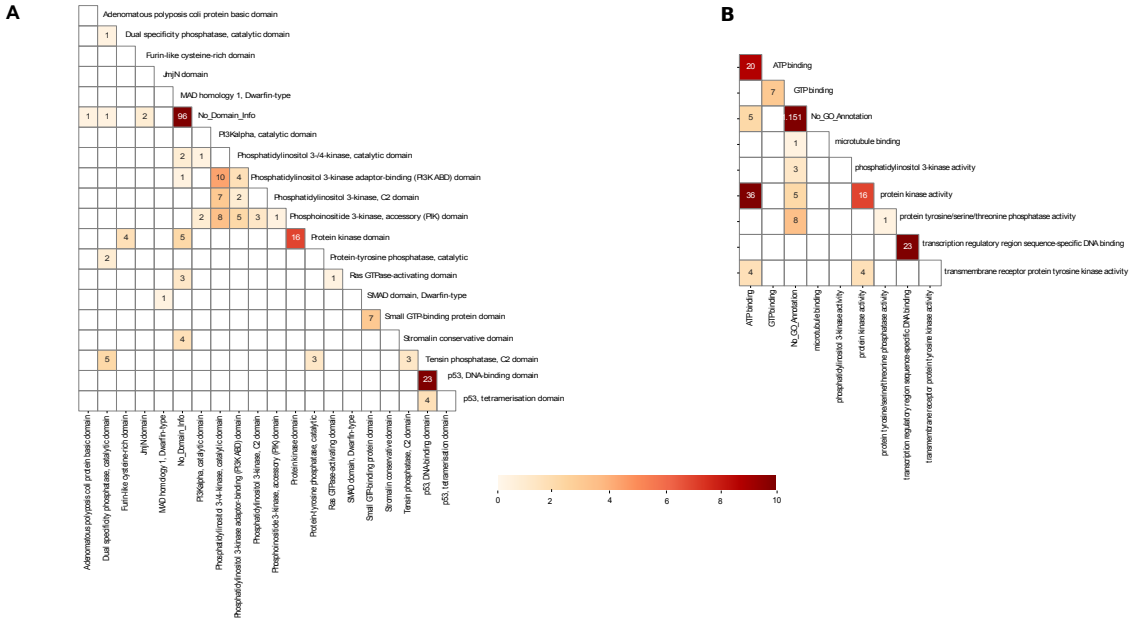

Figure S1. (A) Domain annotation and **(B)** GO molecular function annotation of the mutations in same gene dual mutations. The numbers in the squares correspond to the number of same gene dual mutations where constituents are from the domains on the x and y axes.

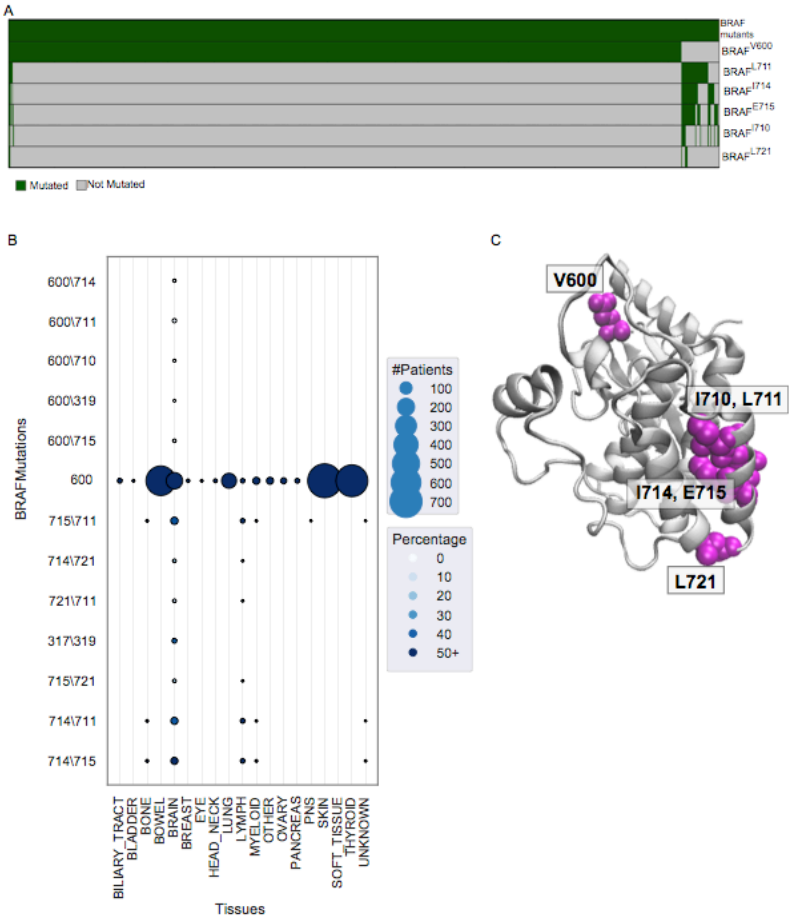

Figure S2 : (A) Oncoprint of frequent BRAF dual mutation constituents. **(B)** Tissue prevalence of dual mutations of BRAF. **(C)** Mutations mapped to 3D structure of BRAF (PDB: 4G9R, Chain: B)

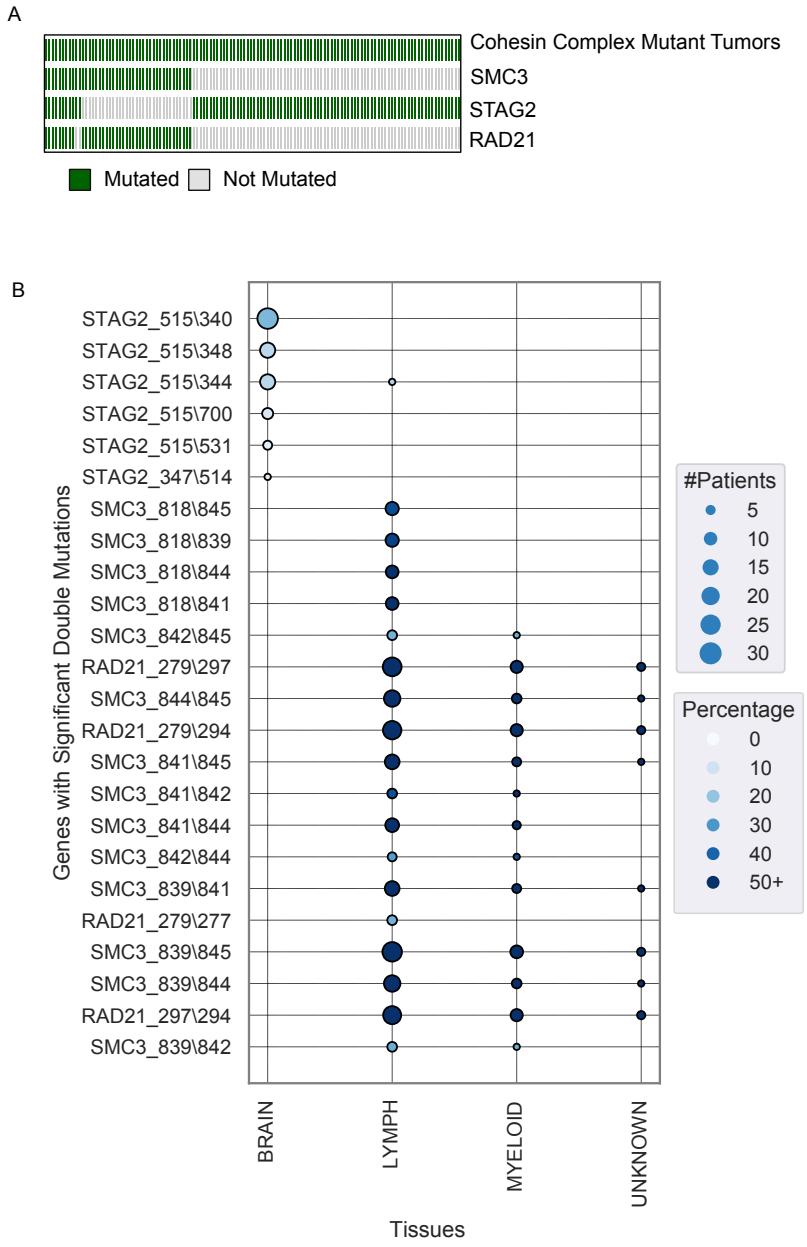

Figure S3 : (A) Oncoprint of Cohesin complex subunits STAG2, RAD21, SMC3. **(B)** Tissue prevalence of dual mutations of STAG2, RAD21, SMC3.

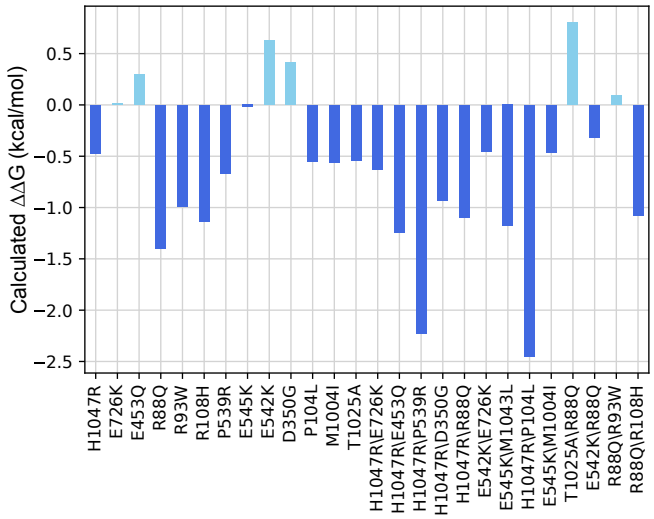

Figure S4: Predicted ΔΔG values for single and dual mutations of PIK3CA calculated with Dynamut web server (PDB id: 4OVV).

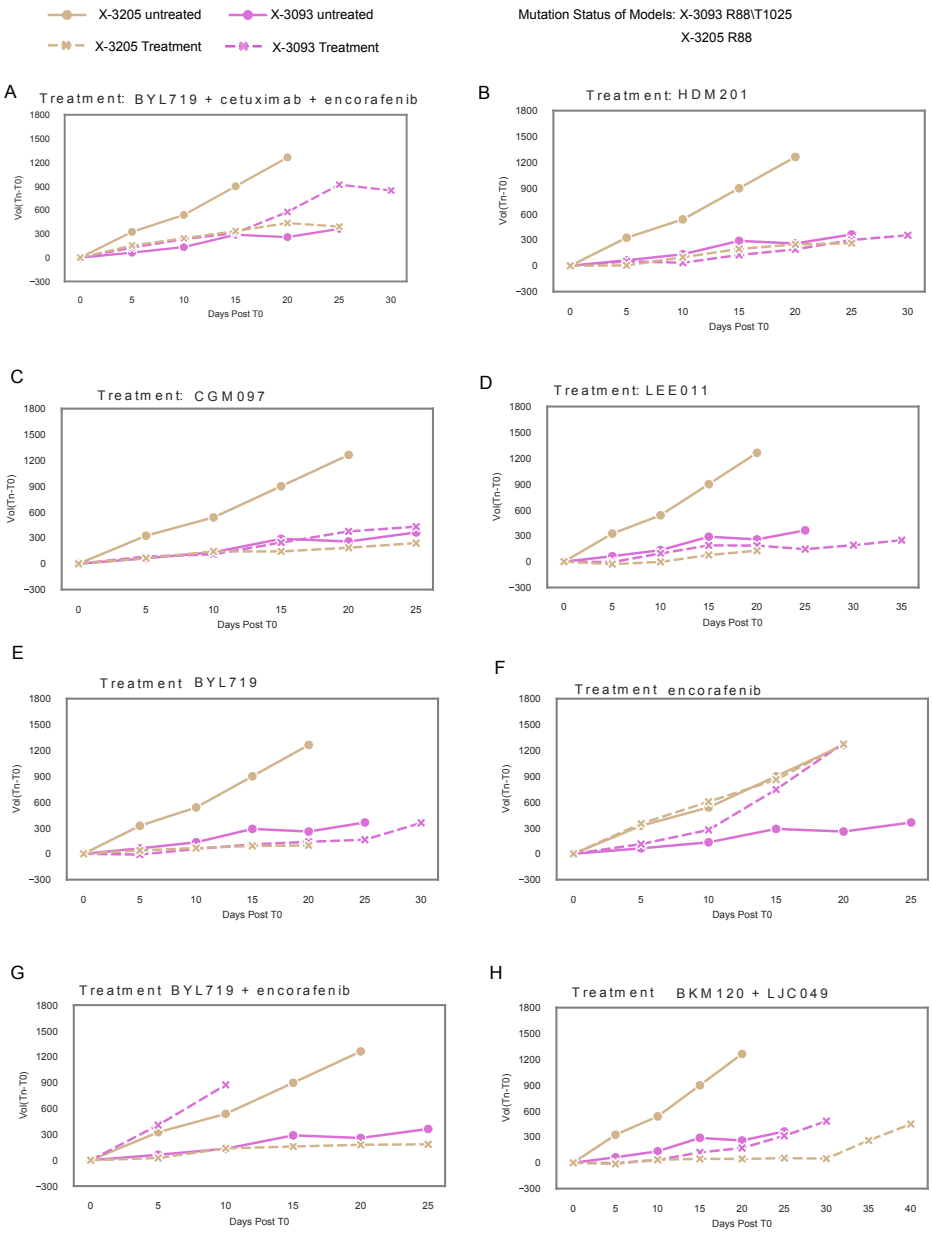

Figure S5. PIK3CA R88\T1025 mutant xenograft (X-3093, BRCA) volume change compared to single R88 mutant xenograft (X-3205, BRCA) for different drug treatments. x-axis shows treatment days, y-axis shows volume difference Volume(Day=n)-Volume(Day=0). Treatment with the drugs/drug combinations **(A)** BYL719+cetuximab+encorafenib combination. **(B)**

HDM201 (Siremadlin). **(C)** CGM097. **(D)**LEE011(**Ribociclib**) **(E)** BYL719 (Alpelisib) **(F)** Encorafenib **(G)** BYL719+Encorafenib

(H) BKM120+LJC049

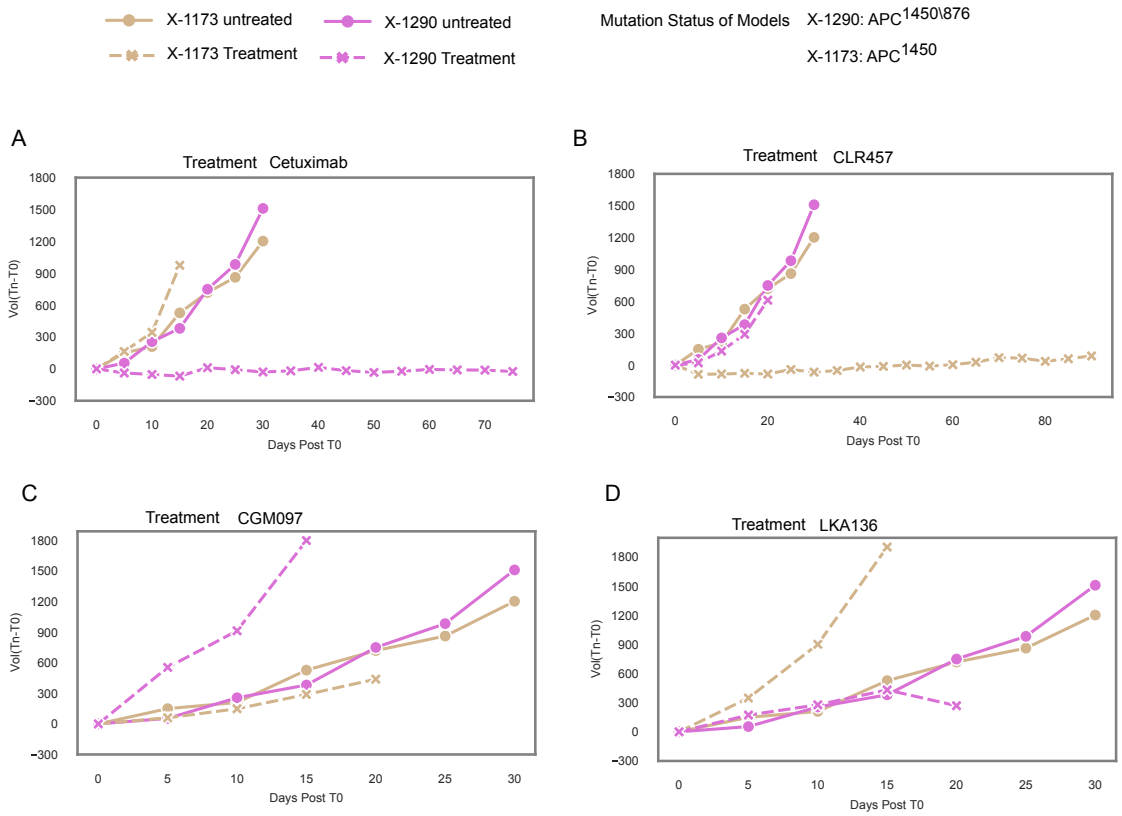

Figure S6. APC R1450\R876 mutant xenograft (X-1290, CRC) volume change compared to single R1450 mutant xenograft (X-1173, CRC) for different drug treatments. x-axis shows treatment days, y-axis shows volume difference Volume(Day=n)-Volume(Day=0). Treatment with the drugs **(A)** Cetuximab **(B)** CLR457 **(C)** CGM097 **(D)** LKA136.

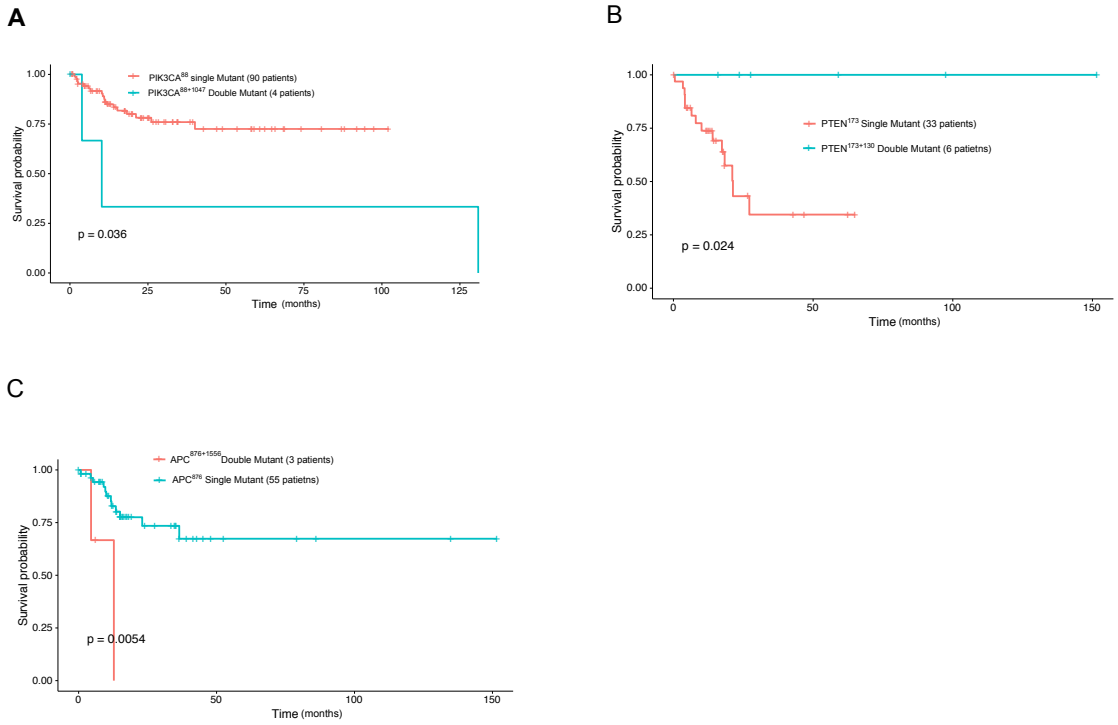

Figure S7. Kaplan-Meier survival analysis comparing single and double mutant patient groups. P-values are calculated with logrank test. **(A)** PIK3CA^{88} and PIK3CA$^{88+1047}$ **(B)** PTEN^{173} and PTEN$^{173+130}$ **(C)** APC^{876} and APC$^{876+1556}$

Supplementary References

1. Chen S, He X, Li R, Duan X, Niu B: **HotSpot3D web server: an integrated resource for mutation analysis in protein 3D structures**. *Bioinformatics* 2020.

2. Meyer MJ, Beltrán JF, Liang S, Fragoza R, Rumack A, Liang J, Wei X, Yu H: **Interactome INSIDER: a structural interactome browser for genomic studies**. *Nature methods* 2018, **15**(2):107.

3. Kuleshov MV, Jones MR, Rouillard AD, Fernandez NF, Duan Q, Wang Z, Koplev S, Jenkins SL, Jagodnik KM, Lachmann A: **Enrichr: a comprehensive gene set enrichment analysis web server 2016 update**. *Nucleic acids research* 2016, **44**(W1):W90-W97.

4. Hunter S, Apweiler R, Attwood TK, Bairoch A, Bateman A, Binns D, Bork P, Das U, Daugherty L, Duquenne L: **InterPro: the integrative protein signature database**. *Nucleic acids research* 2009, **37**(suppl_1):D211-D215.

5. Rodrigues CH, Pires DE, Ascher DB: **DynaMut: predicting the impact of mutations on protein conformation, flexibility and stability**. *Nucleic acids research* 2018, **46**(W1):W350-W355.